

**DEVELOPMENT OF HEK-293T CELLS STABLY
EXPRESSING THE C-X-C CHEMOKINE RECEPTOR TYPE
4 (CXCR4) FOR BINDING ASSAY OF POTENTIAL ANTI-
BREAST CANCER AGENTS**



A Thesis Submitted in Partial Fulfillment of the Requirements
for the Degree of Master of Science in Pharmaceutical Sciences and
Technology
Common Course
FACULTY OF PHARMACEUTICAL SCIENCES
Chulalongkorn University
Academic Year 2021
Copyright of Chulalongkorn University

การพัฒนาเซลล์จากเอ็มบริโอมนุษย์ (เฮค293ที) ที่แสดงออกตัวรับซีเอ็กซ์ซีเคโมไคน์ชนิดที่ 4 (ซีเอ็กซ์ซีอาร์ 4) อย่างคงที่สำหรับการทดสอบสารที่มีศักยภาพในการต้านมะเร็งเต้านม



วิทยานิพนธ์นี้เป็นส่วนหนึ่งของการศึกษาตามหลักสูตรปริญญาวิทยาศาสตรมหาบัณฑิต
สาขาวิชาเภสัชศาสตร์และเทคโนโลยี ไม่สังกัดภาควิชา/เทียบเท่า
คณะเภสัชศาสตร์ จุฬาลงกรณ์มหาวิทยาลัย
ปีการศึกษา 2564
ลิขสิทธิ์ของจุฬาลงกรณ์มหาวิทยาลัย

Thesis Title DEVELOPMENT OF HEK-293T CELLS STABLY
EXPRESSING THE C-X-C CHEMOKINE
RECEPTOR TYPE 4 (CXCR4) FOR BINDING
ASSAY OF POTENTIAL ANTI-BREAST CANCER
AGENTS

By Miss Thi Thai Ha Dinh

Field of Study Pharmaceutical Sciences and Technology

Thesis Advisor Associate Professor PORNCHAI ROJSITTHISAK,
Ph.D.

Thesis Co Advisor Professor OPA VAJRAGUPTA, Ph.D.

Accepted by the FACULTY OF PHARMACEUTICAL SCIENCES,
Chulalongkorn University in Partial Fulfillment of the Requirement for the Master of
Science

..... Dean of the FACULTY OF
PHARMACEUTICAL SCIENCES
(Professor PORNANONG ARAMWIT, Ph.D.)

THESIS COMMITTEE

..... Chairman
(Associate Professor VORASIT VONGSUTILERS,
Ph.D.)

..... Thesis Advisor
(Associate Professor PORNCHAI ROJSITTHISAK,
Ph.D.)

..... Thesis Co-Advisor
(Professor OPA VAJRAGUPTA, Ph.D.)

..... Examiner
(Associate Professor WARANYOO PHOOLCHAROEN,
Ph.D.)

..... External Examiner
(Associate Professor SEIICHI SAKAMOTO, Ph.D.)

ธิ โท ฮา คินห์ : การพัฒนาเซลล์ไคจากเอ็มบริโอมนุษย์ (สค293ที่) ที่แสดงออกตัวรับซีเอ็กซ์ซีเค โทโมไลน์ชนิดที่ 4 (ซีเอ็กซ์ซีอาร์ 4) อย่างคงที่สำหรับการทดสอบสารที่มีศักยภาพในการต้านมะเร็งเต้านม. (

DEVELOPMENT OF HEK-293T CELLS STABLY EXPRESSING THE C-X-C CHEMOKINE RECEPTOR TYPE 4 (CXCR4) FOR BINDING ASSAY OF POTENTIAL ANTI-BREAST CANCER AGENTS) อ.ที่ปรึกษา

หลัก : รศ. ภก. ดร.พรชัย โรจนสีทิสักดิ์, อ.ที่ปรึกษาร่วม : ศ. ภญ. ดร.โอภา วัชรคุปต์

รีเซปเตอร์ซีโมไลน์ C-X-C ชนิด 4 (CXCR4) เป็นเป้าหมายที่มีศักยภาพในการค้นหาตัวยารักษา มะเร็ง เนื่องจากพบว่าเซลล์มะเร็งมีการแสดงออกของรีเซปเตอร์นี้ในปริมาณสูง โดยเฉพาะอย่างยิ่งมะเร็งเต้านมชนิดลุกลาม การศึกษานี้ มีวัตถุประสงค์เพื่อผลิตเซลล์ที่มีการแสดงออกของรีเซปเตอร์ซีโมไลน์ชนิด 4 ในปริมาณสูง สำหรับการคัดกรองสารต้านมะเร็งเต้านมตัวใหม่ที่มุ่งเป้า CXCR4 และการระบุเป้าหมายที่เป็นกลไกในการออกฤทธิ์ของสารต้านมะเร็ง การผลิตเริ่มจากการเพิ่มจำนวนไอโซโทปที่ทางพันธุกรรมของ CXCR4 จำนวน 5 ไอโซโทป คือ A, B, C, D และ E จากเซลล์มะเร็งเม็ดเลือดขาว นำแอมพลิกอนของแต่ละไอโซโทป มาเชื่อมต่อเข้ากับเวกเตอร์โคลนและถูกคัดลอกออกไปเป็นเวกเตอร์การแสดงออก จากนั้นนำเข้าสู่เซลล์เข้าสู่เซลล์ *Escherichia coli* สายพันธุ์ DH5-alpha ทำการตรวจสอบโครงสร้างของยีน CXCR4 ในเซลล์เพื่อคัดลอกโคลนด้วยเทคนิค colony PCR และเจลอดีคโครโฟริซิส พลาสมิดลูกผสมของ CXCR4-ไอโซโทป B ถูกนำไปใช้สำหรับการทรานส์เฟกชันที่เสถียรในเซลล์ HEK293T ทำการตรวจสอบโคลนด้วยวิธีไอโซโทปและเซลล์ที่มีการแสดงออกของ CXCR4 สูงถูกแยกออกโดยใช้เทคนิคการคัดแยกเซลล์ที่กระตุ้นการเรืองแสง ได้เซลล์ HEK293T ที่มีการแสดงออกของ CXCR4 99.8% การตรวจสอบเซลล์ที่มีการแสดงออกของ CXCR4 ทำโดยการนำเซลล์ที่ผลิตขึ้นมาใช้ในการวิเคราะห์การจับแบบแข่งขันกับโมโนโคลนัลแอนติบอดีต้าน CD184 ของมนุษย์ที่ติดฉลากไฟโคอิรีทรินที่เรืองแสง ผลการวิเคราะห์สารต้าน CXCR4 ที่รู้จักดี คือ AMD3100 (เพลริซาฟอรั) ได้ค่า IC₅₀ ของเพลริซาฟอรัในการแข่งขันกับแอนติบอดีเท่ากับ 305.5 นาโนโมลาร์ สอดคล้องกับค่าที่ได้จากการวิเคราะห์การจับแบบแข่งขันกับลิแกนด์ที่มีน้มน้ำมันออกจากนี้ได้นำเซลล์ HEK293T ที่มีการแสดงออกของ CXCR4 สูง มาใช้ในการวิเคราะห์การจับแบบแข่งขันเพื่อระบุเป้าหมายที่ใช้ในการออกฤทธิ์ของสารธรรมชาติซึ่งมีฤทธิ์เป็นพิษต่อเซลล์มะเร็งเต้านม MDA-MB-231 สารธรรมชาติที่นำมาทดสอบเป็นสารสกัดจากสเตฟาเนีย ปีแยร์เร ได้แก่ methoxy-8-uvariopsine, crebanine และ dehydrocrebanine ทั้งนี้การประยุกต์ใช้การทดสอบการจับการแข่งขันกับแอนติบอดีที่ติดฉลากเรืองแสงในการหาการจับของสารธรรมชาติที่มีศักยภาพเหล่านี้มีข้อจำกัดเนื่องจากสารมีการละลายในน้ำต่ำ ทำให้ต้องใช้ตัวทำละลายและสารลดแรงตึงผิวช่วยเพื่อเพิ่มการละลาย ส่งผลให้ความเข้มข้นของการเรืองแสงลดลงเป็นอย่างมาก ดังนั้นจึงจำเป็นต้องมีการพัฒนาต่อในเรื่องตัวทำละลายและสารช่วยละลายที่ไม่รบกวนการเรืองแสงเพื่อให้การทดสอบนี้สามารถใช้เป็นแพลตฟอร์มในการคัดกรอง สารต้านมะเร็งมุ่งเป้า CXCR4 ต่อไป

สาขาวิชา เกษศาสตร์และเทคโนโลยี
ปีการศึกษา 2564

ลายมือชื่อนิสิต
ลายมือชื่อ อ.ที่ปรึกษาหลัก
ลายมือชื่อ อ.ที่ปรึกษาร่วม

6272005633 : MAJOR PHARMACEUTICAL SCIENCES AND TECHNOLOGY

KEYWORD: CXCR4, HEK293T cells, overexpression, flow cytometry, binding assay, anti-breast cancer agents

Thi Thai Ha Dinh : DEVELOPMENT OF HEK-293T CELLS STABLY EXPRESSING THE C-X-C CHEMOKINE RECEPTOR TYPE 4 (CXCR4) FOR BINDING ASSAY OF POTENTIAL ANTI-BREAST CANCER AGENTS.
Advisor: Assoc. Prof. PORNCHAI ROJSITTHISAK, Ph.D. Co-advisor: Prof. OPA VAJRAGUPTA, Ph.D.

The C-X-C chemokine receptor type 4 (CXCR4) has been recognized as a potential target in cancer drug discovery based on the high expression in cancer cells, particularly invasive breast cancer. This study aims to construct CXCR4-overexpressed cells to screen new anti-breast cancer agents targeting CXCR4 and identify the mediated target for anticancer effect. Firstly, five genetic isoforms of CXCR4, namely A, B, C, D and E, were amplified from Jurkat T cells. Amplicons of each CXCR4 isoform were ligated into cloning vectors and subcloned into expression vectors. They were transformed into competent *Escherichia coli* strain DH5- α cells. The presence of CXCR4 plasmids in the selective transformed cells was determined by colony PCR and gel electrophoresis. The recombinant plasmids of CXCR4-isoform B were selected for stable transfection in HEK293T cells. CXCR4 expression was confirmed by flow cytometry and the population of the highly CXCR4 expressing cells was isolated using the fluorescence-activated sorting cells technique to obtain 99.8% of CXCR4-expressing cells. The CXCR4-overexpressed HEK293T cells were verified by conducting the competitive binding assay of a known CXCR4 inhibitor, AMD3100 (plerixafor), using monoclonal anti-human CD184 (CXCR4) antibody tagged with fluorescence probe, phycoerythrin. The obtained IC_{50} of plerixafor (305.5 nM) against the binding of the antibody to CXCR4 was in accordance with those determined by conventional competitive radioligand binding assay. Moreover, the developed CXCR4-overexpressed HEK293T cells were used in the competitive binding assay to identify the mediated target of natural compounds showing high cytotoxicity against the invasive breast cancer cell line MDA-MB-231. The tested compounds were extracted from *Stephania pierrei*, which were methoxy-8-uvариopsine, crebanine and dehydrocrebanine. However, the application of the fluorescence tagged antibody competition binding assay to determine the binding affinity of these potential compounds has been limited due to the poor solubility of natural compounds, which required additional solvent and surfactant to improve the solubility leading to high fluorescence quenching. Further development of low fluorescence quenching solvent and solubilizer is needed to implement this assay in the screening platform.

Field of Study:	Pharmaceutical Sciences and Technology	Student's Signature
Academic Year:	2021	Advisor's Signature
		Co-advisor's Signature

ACKNOWLEDGEMENTS

First of all, I gratefully acknowledged my advisor and co-advisor for allowing me to do the project. Without their support and guidance, the project would not have been accomplished. Assoc. Prof. Pornchai Rojsitthisak and Prof. Dr. Opa Vajragupta have inspired me in research and encouraged me to overcome a difficult time. I would like to express my gratitude to Prof. Dr. Wanpen Chaicumpa at Therapeutic Proteins and Antibody Engineering Laboratory, Siriraj Hospital, Mahidol University for her guidance and kind support.

I am thankful to Dr. Kittirat Glab-ampai, Dr. Kodchakorn Mahasong, Lecturer Dr. Monrat Chulanetra, Mr. Kanasap Kaewchim, and Mr. Techit Thavorasak for all help and guidance when I conduct my thesis experiments in Therapeutic Proteins and Antibody Engineering Laboratory, Siriraj Hospital, Mahidol University.

I always feel grateful when I can study and work with my seniors and classmates in the Department of Food and Pharmaceutical Chemistry, Faculty of Pharmaceutical Sciences, Chulalongkorn University.

I am grateful to my parents for their unconditional love. My parents always believe in and support me during my study time in Thailand.

Last but not least, I would like to thank Thailand Science Research and Innovation Fund Chulalongkorn University under Grant CU_FRB640001_01_33_3 and CU_FRB65_heal (56) 065_33_09, the Ratchadaphiseksomphot Endowment Fund and Graduate Scholarship Program for ASEAN Countries of Chulalongkorn University for financial support.

Thi Thai Ha Dinh

TABLE OF CONTENTS

	Page
ABSTRACT (THAI)	iii
ABSTRACT (ENGLISH).....	iv
ACKNOWLEDGEMENTS	v
TABLE OF CONTENTS.....	vi
LIST OF TABLES	ix
LIST OF FIGURES	x
LIST OF APPENDIX FIGURES.....	1
LIST OF ABBREVIATIONS.....	2
CHAPTER 1. INTRODUCTION	4
CHAPTER 2. LITERATURE REVIEWS.....	6
2.1. Chemokine receptor CXCR4.....	6
2.2. CXCR4/CXCL12 axis role in breast cancer cells.....	7
2.3. CXCR4 antagonists	9
2.3.1. Synthetic compounds	9
2.3.2. Modified peptides.....	10
2.3.3. Natural compounds.....	12
2.4. Aporphine alkaloids.....	13
2.4.1. Boldine	14
2.4.2. Methoxy-8-uvariopsine	14
2.4.3. Crebanine.....	14
2.4.4. Dehydrocrebanine	15
2.5. Production of recombinant chemokine receptor.....	15
2.5.1. Molecular cloning.....	15
2.5.2. Genetic transfection.....	16
2.6. Competitive binding assays	16

2.6.1. Radioligand binding assays	17
2.6.2. Fluorescence-based binding assays	17
3.1. Materials	18
3.1.1. Chemicals and reagents	18
3.2. Methods	19
3.2.1. Tested compounds	19
3.2.2. Cell culture	20
3.2.3. Construction of recombinant CXCR4 plasmids	20
3.2.4. Generation of stable CXCR4-overexpressed cell line.....	22
3.2.4.1. Hygromycin B kill curve/titration	22
3.2.4.2. Stable transfection of CXCR4-pTriEX™ 1.1 Hygro plasmids in HEK293T.....	23
3.2.5. Isolation of CXCR4-overexpressed HEK293T.....	24
3.2.6. Freezing cell stock and mycoplasma contamination test	24
3.2.7. Investigation of CXCR4 expression in HEK293T cells.....	25
3.2.8. Verification of CXCR4-overexpressed HEK293T cells	26
3.2.8.1. Saturation binding assay of PE-conjugated anti-hCD184 antibody	26
3.2.8.2. Competitive binding assay of CXCR4 antagonist (AMD3100)..	26
3.2.9. Determination of binding affinity of natural compounds to CXCR4.....	27
3.2.9.1. Cytotoxicity assay of natural compounds in cancer cell lines.....	27
3.2.9.2. Competitive binding assay of natural compounds	28
3.2.10. Statistical analysis	29
4.1. Production of CXCR4-overexpressed HEK293T cells	30
4.1.1. Recombinant CXCR4 plasmids construction.....	30
4.1.2. Stable CXCR4 expressing HEK293T cells construction	41
4.1.3. The isolation of CXCR4-overexpressed cells	41
4.2. Verification of CXCR4-overexpressed HEK293T cells.....	43
4.2.1. Saturation binding assay using PE-conjugated anti-hCD184 antibody...	44
4.2.2. Competitive binding assay of CXCR4 antagonist.....	44

4.3. Competitive binding assay of natural compounds to CXCR4.....	46
CHAPTER 5. CONCLUSION.....	49
APPENDICES	50
REFERENCES	58
VITA.....	66



LIST OF TABLES

	Page
Table 1. List of synthetic CXCR4 inhibitors	10
Table 2. List of small and cyclic peptide-based CXCR4 inhibitors	12
Table 3. List of natural compound-based CXCR4 inhibitors	13
Table 4. List of chemicals and reagents.....	18
Table 5. Sequences of designed CXCR4 primers	20
Table 6. Master mix preparation for colony PCR.....	21
Table 7. Conditions for the colony PCR reaction	22
Table 8. PCR master mix preparation for mycoplasma contamination test	25
Table 9. PCR condition for mycoplasma contamination test	25
Table 10. The concentrations of natural compounds in different trials	29
Table 11. Positive results of the transformation of CXCR4 isotypes with pJET1.2/blunt vectors into E. coli DH5 α cells using colony PCR technique.....	33
Table 12. The concentration of extracted recombinant CXCR4 plasmids	35
Table 13. Information of reference CXCR4 DNA sequences	36
Table 14. Information of reference CXCR4 protein sequences.....	39
Table 15. IC ₅₀ values of AMD3100 from different competitive binding assays	45
Table 16. The natural compounds of investigation.....	46

LIST OF FIGURES

	Page
Figure 1. Representative CXCR4 protein sequences included the critical residues for CXCR4 for CXCL12-mediated signaling. A total of 41 residues essential for the CXCL12-dependent CXCR4 function are highlighted in red [16].....	6
Figure 2. Signaling pathways mediating tumorigenicity of cancer cells via CXCR4/CXCL12 (or CXCR4/SDF-1 α) axis [20].....	7
Figure 3. The chemical structure of TN14003.....	11
Figure 4. Positions of essential amino acids for binding to CXCR4 receptors [36]...	11
Figure 5. Chemical structures of small cyclic peptides [36-37]	11
Figure 6. The general structure of aporphine alkaloids	14
Figure 7. The designed 96-well plate for competitive binding assay of AMD3100...	27
Figure 8. Production of transfected HEK293T cells stably expressing recombinant CXCR4 for binding assay	30
Figure 9. PCR amplicons of DNA sequences coding for 5 isotypes of CXCR4 (~1000 bp). Lane M: 1 kb DNA ladder marker; Lane A: CXCR4 isotype A amplicon; Lane B: CXCR4 isotype B amplicon; Lane C: CXCR4 isotype C amplicon; Lane D: CXCR4 isotype D amplicon; Lane E: CXCR4 isotype E amplicon. Numbers at the left are DNA sizes in bp.....	31
Figure 10. A flow diagram of the CXCR4 cloning procedure.....	32
Figure 11. Representatives of PCR amplicons of DNA sequences coding for CXCR4 (~1000 bp) from the CXCR4-pJET1.2/blunt plasmids. Lane M: 1 kb DNA ladder marker; Lane 1: Negative control; Lane 2-16: CXCR4 amplicons from E. coli clone 1-15, respectively. Numbers at the left are DNA sizes in bp.....	33
Figure 12. The agarose gel of pTriEX TM 1.1 Hygro vectors after enzyme digestion reaction. Lane M: 1 kb DNA ladder marker; Lane 1: digested pTriEx TM 1.1 Hygro vectors. Numbers at the left are DNA sizes in bp.....	34
Figure 13. The agarose gel of CXCR4-pJET1.2/blunt plasmids after digestion reaction with XhoI and EcoRI restriction enzymes. Lane M: 1 kb DNA ladder marker; Lane 1: digested products of CXCR4-pJET1.2/blunt plasmids of isotypes (a) A9; (b) B6; (c) C2 (d) D1 and (e) E12, respectively, which contain the band of CXCR4 (~1000 bp).....	34

Figure 14. Representatives of PCR amplicons of DNA sequences coding for CXCR4 (~1000 bp) from the CXCR4-pTriEX™ 1.1 Hygro plasmids. Lane M: 1 kb DNA ladder marker; Lane 1: Negative control; Lane 2-11: CXCR4 amplicons from E. coli clones 1-10, respectively. Numbers at the left are DNA sizes in bp.34

Figure 15. The representative alignment results of constructed CXCR4-B DNA sequence with reference DNA sequence (Homo sapiens CXCR4 transcript variant 2_ NM_003467.3) on NCBI database.39

Figure 16. The multiple sequence alignment results of translated CXCR4 DNA sequences with reference protein sequences on the NCBI database. Note: conserved sequence (*); conservative mutations (:) and non-conservative mutations ().....41

Figure 17. Flow cytometric analysis of (a) unstained CXCR4-B expressed HEK293T cells; (b) normal HEK293T cells stained with PE-conjugated anti-hCD184 antibody; (c) pre-sorting CXCR4-B expressed HEK293T cells stained with PE-conjugated anti-hCD184 antibody and (d) CXCR4-overexpressed HEK293T cells sorted by FACS..43

Figure 18. Saturation binding assay of CXCR4 overexpressing HEK293T cells using PE-conjugated anti-hCD184 antibody.44

Figure 19. Competitive binding assay of AMD3100 against PE-conjugated anti-hCD184 antibody.45

Figure 20. Competitive binding assay of crebanine and methoxy-8-uvariopsine diluted in PBS using PE-conjugated anti-hCD184 antibody and CXCR4-overexpressed HEK293T cells. The concentration of reference CXCR4 antagonist (AMD3100) and clonidine was 305.5 nM48

LIST OF APPENDIX FIGURES

	Page
Figure A1. BLAST results of CXCR4-A sequence.....	50
Figure A2. BLAST results of CXCR4-B sequence.....	50
Figure A3. BLAST results of CXCR4-E sequence.....	51
Figure A4. BLAST results of CXCR4-C sequence.....	51
Figure A5. BLAST results of CXCR4-D sequence.....	52
Figure A6. Mycoplasma contamination test of CXCR4-B-overexpressed HEK293T cells. Lane M: GeneRuler™ 100 bp DNA ladder; Lane 1: Positive control (DNA of Mycoplasma bacteria); Lane 2: Negative control (Nuclease-free water); Lane 3-5: Negative results of CXCR4-B overexpressed HEK293T clone 1-3, respectively. Numbers at the left are DNA sizes in bp.....	52
Figure A7. Gating strategy is shown in forward and side scatter with 82.8% intact HEK293T cells in Isotype control (isotype R α -His); Flow cytometry analysis of HEK293T cells incubated with isotype R α -His at 1:200 dilution....	53
Figure A8. Flow cytometry analysis of HEK293T cells transient transfected with CXCR4 isotype A9, B6, C2, D1 and E12 respectively incubated with anti-CXCR4 antibody [UMB2] at 1:200 dilution (a, b, c, d and e); Flow cytometry analysis of HEK293T cells incubated with isotype R α -His at 1:200 dilution (f).....	54
Figure A9. Results of competitive binding assays of crebanine and PE-conjugated anti-hCD184 antibody in CXCR4-overexpressed HEK293T cells...	55
Figure A10. Results of competitive binding assays of methoxy-8-uvariopsine and PE-conjugated anti-hCD184 antibody in CXCR4-overexpressed HEK293T cells.....	56
Figure A11. Results of competitive binding assays of dehydrocrebanine and PE-conjugated anti-hCD184 antibody in CXCR4-overexpressed HEK293T cells.....	57

LIST OF ABBREVIATIONS

AC: adenylate cyclase

AKT: protein kinase B

APC: allophycocyanin

Ca²⁺: calcium

cAMP: cyclic adenosine monophosphate

CCRF-CEM: T lymphoblastoid cell line

CHO: Chinese hamster ovary cell line

CXCR4: C-X-C chemokine receptor type 4

CXCL12: C-X-C ligand type 12

EC₅₀: the half-maximal effective concentration

ER: estrogen receptor

ERK1/2: extracellular signal-regulated kinase 1/2

FITC: fluorescein isothiocyanate

GPCRs: guanine protein-coupled receptors

GRK: guanosine-protein receptor kinase

HEK293T: human embryonic kidney 293 T cell line

HER-2: human epidermal growth factor receptor 2

IC₅₀: the half-maximal inhibitory concentration

K_i: binding affinity

Jak: Janus kinase

MAPK: mitogen-activated protein kinase

mTOR: mechanistic target of *Rapamycin*

NF- κ B: nuclease factor-kappa B

PE: phycoerythrin

PI3K: phosphatidylinositol-3-kinase

PKA: protein kinase A

PKC: protein kinase C

PLC: phospholipase

PR: progesterone receptor

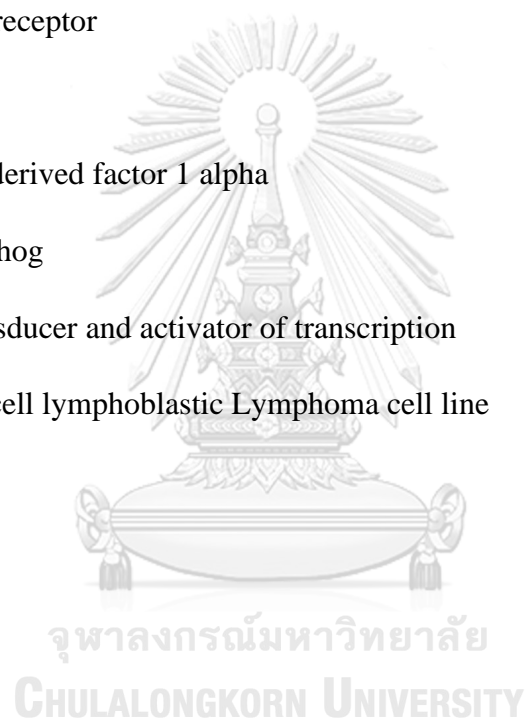
Ras: Ras protein

SDF-1 α : stromal-derived factor 1 alpha

SHH: sonic hedgehog

STAT: signal transducer and activator of transcription

SupT1: human T cell lymphoblastic Lymphoma cell line



CHAPTER 1. INTRODUCTION

Chemokine receptors are the typical cell surface heterotrimeric guanine protein-coupled receptors (GPCRs), which are implicated in inflammation of immune diseases and the development of cancers. Among most concerned chemokine receptors, C-X-C receptor type 4 (CXCR4), also called fusin or CD184, has been early found to be the major co-receptor with CCR5 on CD4 positive (CD4⁺) T-cells for binding of human immunodeficiency virus type 1 (HIV-1) strains and show the impact on the efficiency of viral infection [1-2]. The overexpression of CXCR4 has been found in more than 23 types of cancers, particularly breast cancer, especially in metastasis tumors. The axis of CXCR4 and its cognate chemokine ligand CXCL12 (CXCR4/CXCL12 axis) regulates cancer cell proliferation, metastasis and angiogenesis and plays a crucial role in tumor microenvironment cross-talk in several solid tumors [3]. Therefore, CXCR4 antagonists including small modified peptides and small molecules have been investigated in searching for anti-cancer drugs targeting CXCR4 [4-6].

Chemotherapy is a type of cancer treatment that uses one or more anti-cancer drugs. The conventional anti-cancer drugs commonly used are non-target drugs that cause severe complications and side effects and relates to drug resistance phenomena. This has led to an increase in studies on natural compounds as an alternative in recent decades. Thus, screening for new potential anti-cancer agents derived from medicinal plants targeting CXCR4 is needed. Most experimental screenings for anti-cancer drugs nowadays use cytotoxicity assay to identify potential compounds in which the mechanism-mediated cytotoxicity or drug target has not been assessed. The target-based assay is necessary for providing an insight into the mechanism of action.

In this study, natural compounds showing cytotoxicity against invasive breast cancer cell lines were investigated for target-mediated cytotoxicity. The selected compounds were methoxy-8-uvариopsine, crebanine and dehydrocrebanine from *Stephania pierrei*. Since highly expression of CXCR4 was found in breast cancer, particularly in triple-negative breast cancer, the mechanism of CXCR4 mediated cytotoxicity of these natural compounds has yet to be demonstrated.

For rapid evaluating the pharmacological properties of multiple receptors and screening the interaction between receptors and their ligands, the production of recombinant proteins is a crucial step [7]. Regarded as the first-choice vehicle for the expression of many human recombinant proteins, HEK293 cell lines have been used to analyze several chemokine receptors [7-9]. Therefore, molecular cloning and stable transfection of the CXCR4 gene in eukaryotic cells, HEK293T cells were carried out. The produced CXCR4-overexpressed HEK293T cells can be used as a tool in a target-based assay for target identification and determination of binding affinity. Moreover, they can be used for screening potential anti-cancer agents targeting CXCR4 receptor overexpression in solid tumors.

This research hypothesizes that the CXCR4-overexpressed HEK293T cells can be valuable tools for evaluating molecular mechanisms via CXCR4 by binding assay of potential anti-cancer agents to CXCR4-overexpressed cells. The natural compounds such as methoxy-8-uvariopsine, crebanine and dehydrocrebanine showing cytotoxic effects in breast cancer lines that highly express CXCR4 may mediate the cytotoxic effects through CXCR4 in the binding assays using CXCR4-overexpressed HEK293T cells.

The research work included the construction of recombinant CXCR4 plasmids and transfected the constructed plasmids to the HEK293T cells. The verified CXCR4-overexpressed HEK293T cells were used to determine the binding affinity of the selected herbal compounds to the CXCR4.

CHAPTER 2. LITERATURE REVIEWS

2.1. Chemokine receptor CXCR4

As a GPCR, C-X-C receptor type 4 (CXCR4) comprises an extracellular N-terminus connected with seven transmembrane alpha (α)-helices and an intracellular C-terminus in the structure [10]. The α -helices are linked by three intracellular loops and three extracellular loops. Different isoforms of CXCR4 have been characterized based on the encoding of alternate transcriptional splice variants. However, the CXCR4-B isoform (352 amino acid residues) is considered as a canonical sequence and expressed abundantly in nature. CXCR4 in humans has 89% similarity compared to CXCR4 in mice (359 amino acid residues), and they both express in embryonic and mature tissues [5, 11-12]. Mutation studies have considered that the N-terminus and three extracellular hydrophilic loops of CXCR4 contribute to chemokine binding. In contrast, the binding pocket composed of transmembrane α -helices helps to activate the receptor and enhance the binding affinity of receptors and ligands [5, 13-14]. On the other hand, mutations involved in C-terminus truncations have been found to associate with warts, hypogammaglobulinemia, infections, and myelokathexis (WHIM) syndrome [5, 15].

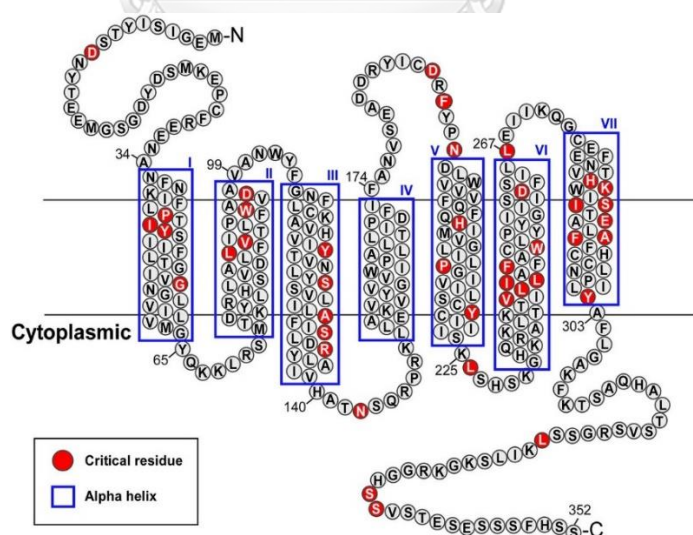


Figure 1. Representative CXCR4 protein sequences included the critical residues for CXCR4 for CXCL12-mediated signaling. A total of 41 residues essential for the CXCL12-dependent CXCR4 function are highlighted in red [16]

To date, C-X-C chemokine type 12 (CXCL12, or stromal cell-derived factor-1 (SDF-1), macrophage migration inhibitory factor (MIF) and ubiquitin have been found as the endogenous ligands of CXCR4 [17-19]. The cognate interaction between CXCR4 and CXCL12 is well-known in various cell types including cancer cells. As shown in Figure 2, they activate multiple downstream signaling pathways such as PI3K-AKT, PLC-Ca²⁺, Ras-MAPK, and Jak-STAT for chemotaxis, proliferation and gene transcription of cancer cells. Other pathways relating to stem cells, such as Wnt/ β -catenin, SHH-GLI-NANOG, Notch, contributed to CXCR4 expression and led to the proliferation and invasion of cancer cells [20].

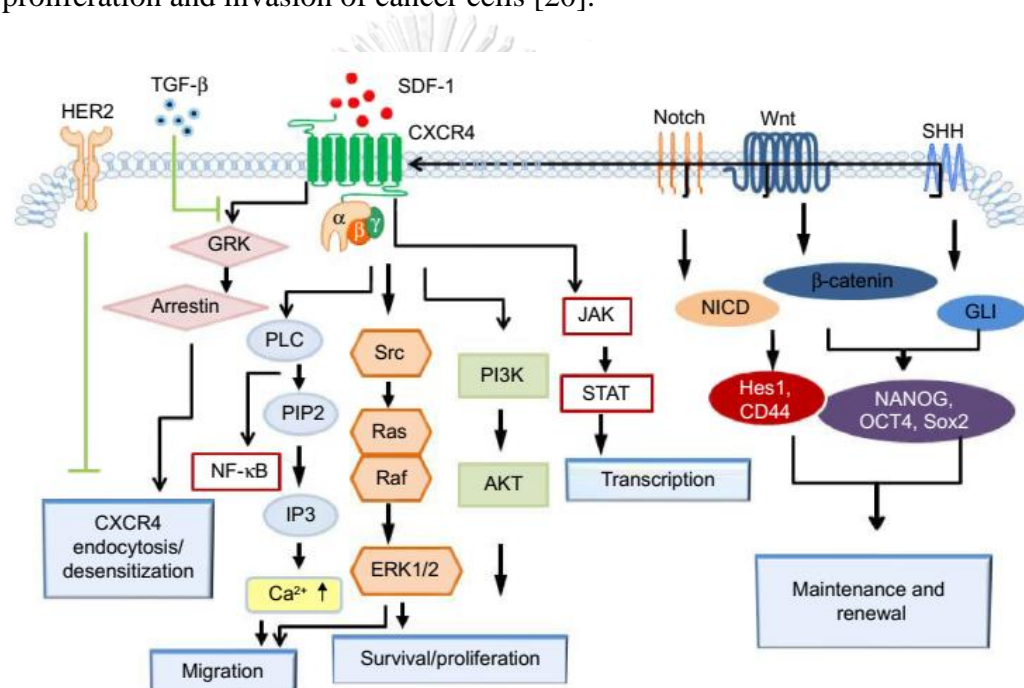


Figure 2. Signaling pathways mediating tumorigenicity of cancer cells via CXCR4/CXCL12 (or CXCR4/SDF-1 α) axis [20]

2.2. CXCR4/CXCL12 axis role in breast cancer cells

Breast cancer is the leading diagnosed heterogeneous disease in women worldwide [21]. In recent years, the disease incidence rate in women has tended to increase slightly, which is considered to come from the decline of fertility rate and the increase of body weight [22]. After a long-term decline, the downward trend of death rate by breast cancer has slowed [22]. Many risk factors generate the disease, including non-modified and modified risk factors. Non-modified factors include

gender, age, heredity and family history of breast cancer [23]. Other factors such as non-physical activity, obesity, reproductive history, using hormone replacement therapy, drinking alcohol, smoking, exposure to chemicals or radiation are considered as modified factors [23]. According to the US Centers for Disease Control and Prevention (CDC), breast cancer is defined as the cluster of over-grow cells and begin in any part of the breast. Common breast cancers are primarily found in lobules and ducts, such as invasive lobular carcinoma, ductal carcinoma and ductal carcinoma in situ (DCIS). In breast cancer, estrogen receptor (ER), progesterone receptor (PR), human epidermal growth factor receptor 2 (HER2) are primary receptors that have been determined. There are three main subtypes of breast cancer: luminal tumor, HER-2 enriched tumor and basal-like tumor. Luminal tumors express ER and/or PR positively, whereas basal-like tumors lack the hormone receptors and HER-2 [24]. In addition, the majority of basal-like cancers are accounted for triple-negative breast cancers (TNBC).

In the research of Muller et al. (2001) [25], the CXCR4 receptor was first described as involved in solid cancer dissemination and highly expressed in malignant breast tumors and metastases. At the transcription level, the binding of hypoxia-inducible factor 1 alpha (HIF-1 α) and HIF-2 to respond to the hypoxia in the tumor as well as the binding of NF- κ B in CXCR4 gene promoter that induce the transcription of CXCR4 and subsequently activate the CXCR4/CXCL12 signaling pathways [20]. In addition, the stabilized HIF-1 α in the hypoxia state leads to CXCR4 expression and activates the expression of vascular endothelial growth factor (VEGF) genes. A high VEGF level is considered that promotes metastasis and angiogenesis of breast cancer by two action manners (i.e., paracrine and autocrine manners) [20]. At the posttranscriptional and translational levels, like other solid tumors, CXCR4 and the CXCR4/CXCL12 axis activate multiple signaling pathways that contribute to cancer progression, cancer invasion and distant metastasis [6, 20, 26]. In the tumor environment, stromal fibroblasts, endothelial cells and immune cells are non-cancerous cells that are connected with connective tissue and extracellular matrix and support tumor structure, angiogenesis and tumor growth [26]. CXCL12 has been found highly expressed in cancer cells and stromal cells associated with tumors [20].

Therefore, it stimulates tumor proliferation and invasion by attracting inflammatory factors, vascular and stromal cells into the tumor mass [26]. Subsequently, they contribute to tumor growth by releasing pro-angiogenic and tumor-growth factors, cytokines and chemokines. In breast tumor tissues, they have shown some level of CXCR4 expression. It increases with the differentiation of tumor (or tumor grade) in normal breast tissue (20%), ductal carcinoma in situ (43%) and invasive breast tissue (67%) [27]. It is also upregulated in HER-2 negative breast tumors and is more likely to increase aggressiveness and recurrence [28]. According to the research of Chu et al. (2010), CXCR4 is highly expressed in nearly 75% of TNBC patients [29].

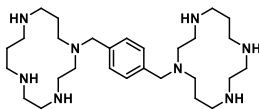
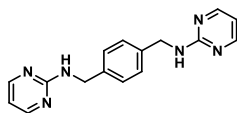
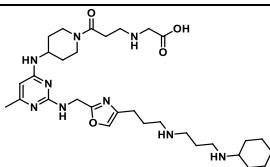
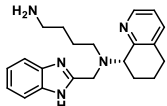
2.3. CXCR4 antagonists

Several CXCR4 antagonists have been developed as potential candidates for cancer chemotherapy. The CXCR4 antagonists are categorized based on the structures as follows.

2.3.1. Synthetic compounds

The design of the synthesis of the CXCR4 antagonist was started in 1990. The first generation of CXCR4 antagonists is bicyclam analogs. Plerixafor (AMD3100) is the first CXCR4 antagonist approved by the US-FDA and used as a mobilizer of hematopoietic stem cells in cancer patients [30]. However, AMD3100 has limitations in treating solid tumors because of toxic side effects and poor pharmacokinetics in long-term use [31]. The 2nd and 3rd generation analogs based on AMD3100 and AMD070, novel mono and bicyclic heterocycles ureas and guanidines, have been investigated [30]. The synthetic compounds as the CXCR4 antagonists or inhibitors are listed in Table 1.

Table 1. List of synthetic CXCR4 inhibitors

Code name	Structure	Biological activities	Study profile	Ref
AMD3100 + bevacizumab	-	Prevent the growth of glioblastoma cells	NCT01339039 (Phase 1)	*
AMD3100		Inhibit the growth of Ewing sarcoma, neuroblastoma, brain tumors	NCT01288573 (Phase 1, 2)	*
MSX-112		Inhibit the growth refractory metastatic or locally advanced solid tumors	NCT00591682 (Phase 1)	*
BPRCX807		Inhibit migration and metastasis in hepatocellular carcinoma cells	Preclinical (in vitro, in vivo)	[31]
AMD070 (Mavorixafor)		Block HIV entry CXCR4 antagonist	Phase I	[32]

(Note: [*] Based on the clinical trial number and study phase of drugs on clinicaltrials.gov website)

2.3.2. Modified peptides

Peptide-based CXCR4 antagonists were designed based on the natural ligand and polyphemusin I and II discovered from horseradish extracts. The polyphemusin was initially used in the treatment of HIV [33]. However, this peptide had toxicity and low efficiency, and it was further developed to TN14003. TN14003 comprises 14 amino acids bound by peptide bonds and has the S-S bond between positions 4 and 13 (Figure 3) [34]. TN14003 has a high inhibitory effect on the CXCR4 receptor with reasonable specificity and has low toxicity. However, it has poor pharmacokinetic properties. They are also very stable in biological fluids and further developed into cyclic peptides [35].

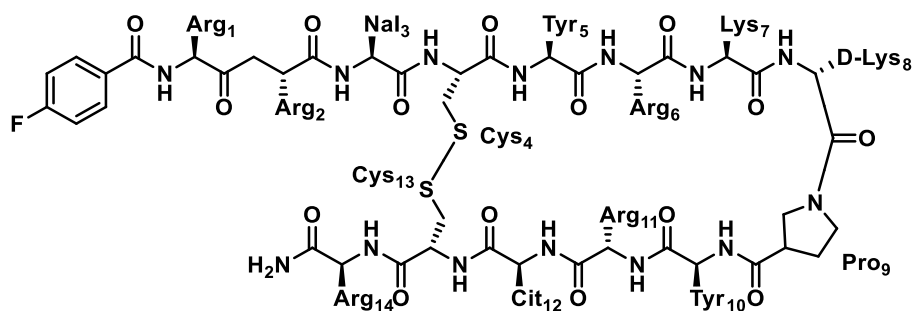


Figure 3. The chemical structure of TN14003

The cyclic peptides were developed from TN14003 by studying the position of essential amino acids and eliminating unnecessary parts. The critical amino acid residues of TN14003 that interact with the CXCR4 receptor were four amino acids at positions 2, 3, 5 and 14 (Figure 4) [36]. The design was then coiled by four amino acids to form a new structure called a small cyclic peptide (Figure 5) [36-37]. In Table 2, several small peptides and cyclic peptides were developed as CXCR4 inhibitors.

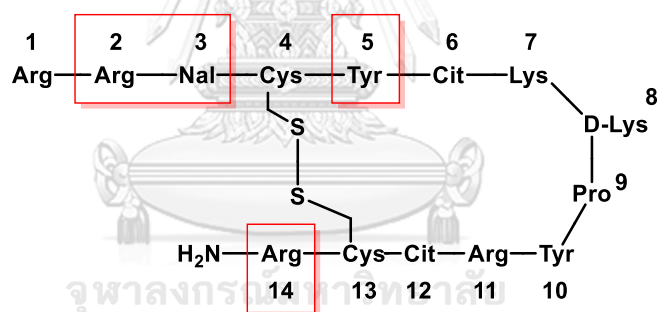


Figure 4. Positions of essential amino acids for binding to CXCR4 receptors [36]

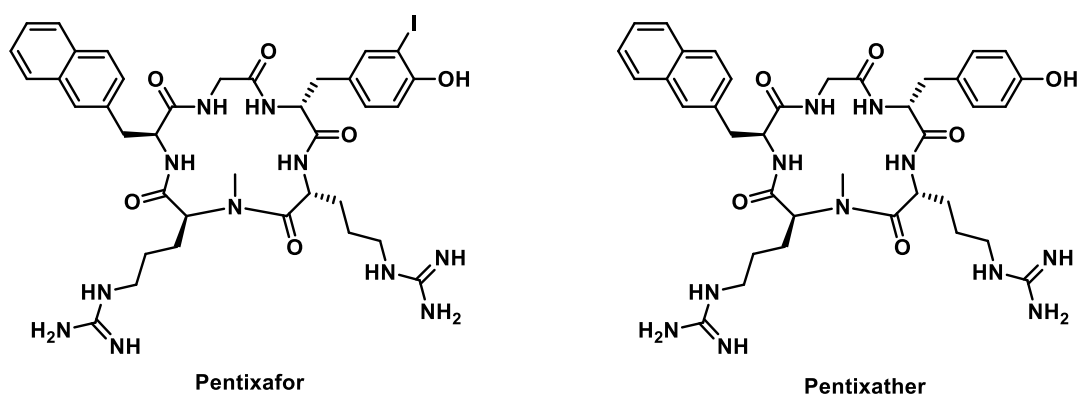


Figure 5. Chemical structures of small cyclic peptides [36-37]

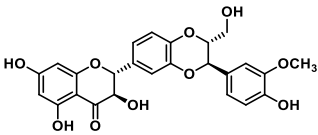
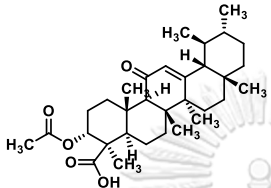
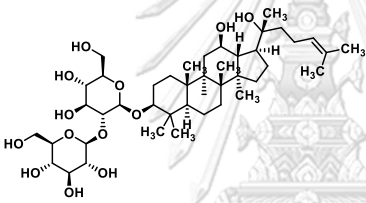
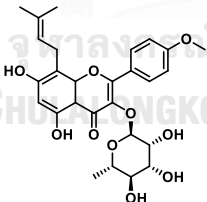
Table 2. List of small and cyclic peptide-based CXCR4 inhibitors

Code name	Structure	Biological activities	Study profile	Ref
CCIC16		<ul style="list-style-type: none"> Block HIV entry CXCR4 antagonist 	Preclinical (in vitro, in vivo)	[33]
FBn-TN14003		<ul style="list-style-type: none"> Block HIV entry CXCR4 antagonist 	Preclinical (in vitro, in vivo)	[34]
T22	$\text{H}_2\text{N}-\text{RRWCYRKCYKGYCRKCR}-\text{CONH}_2$	<ul style="list-style-type: none"> Block HIV entry Anti-RA activities 	Preclinical (in vitro, in vivo)	[38]
CTCE-9908	KGVLSLYRKRYLSLVGK	<ul style="list-style-type: none"> Inhibit cancer growth and metastases 	Phase II	[39]
FC131 (Pentixafor)		<ul style="list-style-type: none"> Block HIV entry Anti-RA activities CXCR4 antagonist 	Preclinical (in vitro, in vivo)	[36, 40]
Pentixather		<ul style="list-style-type: none"> Block HIV entry Anti-RA activities CXCR4 antagonist 	Preclinical (in vitro, in vivo)	[36-37]

2.3.3. Natural compounds

Natural compounds have shown the safety and the potency to be alternatives for chemically synthesized drugs when they possess many pharmacological activities, especially anti-cancer activities and less system toxicity. Several natural compounds have been investigated to downregulate the overexpression of CXCR4 in cancer cells (Table 3). However, only a few CXCR4 antagonists have been evaluated under clinical trials for treating CXCR4 implicated cancers.

Table 3. List of natural compound-based CXCR4 inhibitors

Code name	Structure	Biological activities	Study profile	Ref
Silibinin		<ul style="list-style-type: none"> Inhibit migration and invasion of breast cancer cells via AKT-ERK pathways induced by CXCL12 	Preclinical (in vitro)	[41]
Acetyl-11-keto- β -boswellic acid (AKBA)		<ul style="list-style-type: none"> Suppress the CXCL12-induced invasion of pancreatic cancer and breast cancer cells 	Preclinical (in vitro)	[21]
Ginsenoside Rg3		<ul style="list-style-type: none"> Inhibit CXCR4 expression in metastatic breast cancer cell lines at a non-cytotoxic dosage Decrease the cancer migration and invasion induced by CXCL12 in wound healing assay 	Preclinical (in vitro)	[42]
Baohuoside I		<ul style="list-style-type: none"> Suppress the CXCR4 transcription in prostate cancer, myeloma, osteosarcoma, and skin cancer cells Inhibited CXCL12-induced invasion of cervical cancer and breast cancer cells 	Preclinical (in vitro)	[43]

2.4. Aporphine alkaloids

Aporphine alkaloids are tetracyclic compounds, grouping as a subset of the tetrahydroisoquinoline (or benzyloisoquinoline) alkaloids and contain a single chiral center at position C6a (Figure 6) [44]. More than 500 compounds have been reported and isolated from many plant families [45]. In natural aporphines, the C1 and C2 positions are always substituted by hydroxyl, methoxy or methylenedioxy groups.

They also are present at positions C9, C10 and C11, less frequently at C3 and C8 and C4 or C7 is oxygenated in a few cases [46].

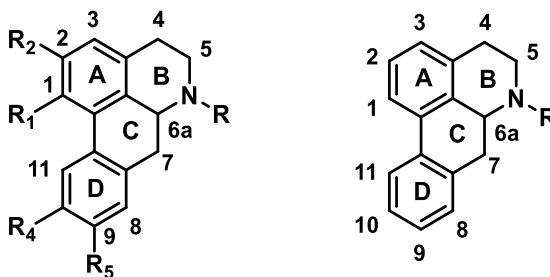


Figure 6. The general structure of aporphine alkaloids

2.4.1. Boldine

Boldine is an aporphine alkaloid characterized by a high polyphenol content and found in many parts of the *Peumus boldus*, such as leaves, bark and roots. It has shown anti-oxidant, anti-inflammatory properties and anti-proliferative response in cancer cells [47]. It was proved to induce apoptosis pathways in bladder cancer cells [48] and possess protective effects against rat hepatocarcinoma in the in vivo study [49]. According to the study of Paydar et al. [50], cytotoxic effects of boldine have been investigated on human invasive breast cancer cells with the half-maximal inhibitory concentration (IC_{50}) of $46.5 \pm 3.1 \mu\text{g/mL}$ (MDA-MB-231) and $50.8 \pm 2.7 \mu\text{g/mL}$ (MDA-MB-468) after 48 hours (hrs), respectively. Moreover, boldine has shown antitumor activity by reducing the tumor size of breast adenocarcinoma cells on in vivo rat models [50].

2.4.2. Methoxy-8-uvariopsine

Methoxy-8-uvariopsine, an aporphine alkaloid, was first isolated from the bark of *Uvariopsis guineensis* Keay and described in research of Leboeuf et al. in 1972 [51]. This compound has been found in *Stephania pierrei* Diels [52]. However, their anti-cancer activity has yet investigated so far, except in this study.

2.4.3. Crebanine

Crebanine is an aporphine alkaloid commonly found in *Stephania* genus. In the research of Wongsirisin, crebanine isolated in *Stephania venosa* significantly

inhibited the proliferation of human cervix cancer cell lines and leukemia and fibrosarcoma cells via the G0/G1 cell cycle arrest and apoptosis mediation [53]. It also inhibits the proliferation of lung, breast and ovarian cancer cells via reducing NF- κ B activity and expression of proteins regulated by NF- κ B [54]. Crebanine also mediated the alpha-7 nicotinic acetylcholine receptor and enhance the memory and cognition on mice [55].

2.4.4. Dehydrocrebanine

Dehydrocrebanine has been found in *Stephania* genus and demonstrated anti-cancer activity on several cancer cells. Dehydrocrebanine isolated from *Stephania glabra* (Roxb.) Miers was reported to have significant cytotoxic effects on cell lines of human ovarian carcinoma (OVCAR-8) and breast adenocarcinoma (MDA-MB-231) with IC₅₀ of 1.38 ± 0.05 μ g/mL and 5.00 ± 0.03 μ g/mL, respectively [56]. It showed the strong cytotoxicity effect to promyelocytic leukemia cells (HL-60), cholangio carcinoma (HUCCA-1), acute lymphoblastic leukemia (MOLT-3) and breast cancer (BC) cells [57].

2.5. Production of recombinant chemokine receptor

2.5.1. Molecular cloning

Molecular cloning of an interest protein or specifically chemokine receptor allows rapid research about its structure, function, expression or regulation and evolution. There are three common elements required for cloning a chemokine receptor: a library of cloned DNA, transfection method and function assays to examine the relevant clone. Two basic choices for constructing a DNA library: (1) total genomic DNA extracted from cells in an organism of interest and (2) complementary DNA from poly-A-tail tagging RNA of a cell type known to produce a receptor of interest [58]. Plasmids or bacterial virus vectors and bacterial competent cells such as *E. coli* are main components for cloning of gene coding receptor of interest.

2.5.2. Genetic transfection

Genetic transfection plays an essential role in linking genomics and proteomics studies aiming to study the function of genes or gene products. It is useful for analyzing the regulation of gene expression and production of recombinant proteins by introducing foreign genetic materials into the eukaryotic cells or the animal models [59]. The genetic materials can be DNA, RNA, messenger RNA, small interfering RNA, microRNA and short hairpin RNA [60]. There are two types of gene transfection, namely transient and stable transfection. Transient transfection is when the introduced gene is not integrated into the host cell genome and is only expressed quickly. In contrast, stable transfection is in which the introduced gene is either integrated into the genome of the host cell or maintained in episomal form (also called circular extrachromosomal DNA or plasmid) [59-60]. For stable transfection, antibiotic resistance genes on the introduced genetic material can be used as markers for selecting the cells that have genome integrated with the transfected gene or carry the transfected gene to generate a cell line stably expressing the gene of interest [59-60]. Therefore, the technique helps test interaction between the selective probes and targeting proteins of interest.

2.6. Competitive binding assays

The competitive binding assay is a technique used to determine binding affinity between a drug and its targets such as receptor and enzyme. The binding affinity is an essential pharmacodynamic property to explain how the drug exerts pharmacological action and potency. The common methods used in the competitive binding assays are presented as follows.

In a competitive binding assay, the binding affinity (K_i) of a non-labeled ligand to a receptor can be determined in the presence of a labeled ligand [61-62]. The K_i value can be calculated via the Cheng-Prusoff transformation equation [61, 63]. Therefore, the increasing concentration series of potential compounds will be tested in a fixed concentration of the labeled probe. The compounds that interfere with the probe binding to the receptor will decrease the signal from the probe.

The Cheng-Prusoff transformation equation:

$$K_i = \frac{IC_{50}}{1 + \frac{[L]}{K_d}}$$

[L]: the free concentration of the labeled ligand

K_i : the equilibrium inhibitor constant (or binding affinity) of the non-labeled compound

K_d : the equilibrium dissociation constant (or affinity constant) of the labeled ligand

IC_{50} : the concentration of non-labeled compound which inhibits 50% specific binding of the labeled ligand.

2.6.1. Radioligand binding assays

Radioligand binding assays have been developed to measure ligand binding affinity to a target receptor for a long time. It has shown robustness and sensitivity. Radioligand binding assays include three main types: competitive, saturation and kinetic assays. For competitive binding assay, the relative affinities (K_i values) of test compounds bind to receptor sites on cells is determined by radioactive signals from a radioligand. Particularly, a range of concentrations of unlabeled compounds with a fixed concentration of radioligand is performed, and IC_{50} of tested compounds is determined.

2.6.2. Fluorescence-based binding assays

In previous studies, most binding assays used radioactive-labeled ligands or antibodies as competitive materials to evaluate their binding affinities to a receptor. However, this is not user-friendly, with poor stability and high background signals [64]. Thus, a fluorescent labeling approach is developed to reduce the harm of radioactive materials.

CHAPTER 3. RESEARCH METHODOLOGY

3.1. Materials

3.1.1. Chemicals and reagents

Table 4. List of chemicals and reagents

Chemicals and reagents	Origin
Agarose	Omnipur- Merck KGaA, Germany
Agar powder	Himedia, India
AMD3100 (plerixafor)	Biotek Abadi SDN, Malaysia
Ampicillin (250 mg/mL)	-
Boldine	Santa Cruz Biotechnology
Bovine serum albumin	Sigma-Merck KGaA, Germany
CloneJET PCR cloning kit	Thermo Fisher Scientific, USA
Clonidine hydrochloride (Clonidine.HCl)	Tocris Bioscience, UK
Deionized water	-
Dimethyl sulfoxide	Sigma-Merck KGaA, Germany
Dulbecco's modified Eagle's medium	Thermo Fisher Scientific, USA
Dulbecco's phosphate-buffered saline	Thermo Fisher Scientific, USA
Ethylenediaminetetraacetic acid (EDTA)	KEMAUS, Australia
FACS buffer (2% FBS, 0.02% NaN ₃ in PBS)	Sigma-Merk KGaA, Germany
FastDigest restriction enzymes kit	Thermo Fisher Scientific, USA
Favorprep kit	Favorgen, Taiwan
Fetal bovine serum	Thermo Fisher Scientific, USA
GenepHlow™ gel/PCR kit	Geneaid, Taiwan
GeneRuler™ 1kb DNA ladder	Thermo Fisher Scientific, USA
GeneRuler™ 100 bp DNA ladder	Thermo Fisher Scientific, USA
Glacial acetic acid	Qrec, New Zealand
Glycerol (80%)	KEMAUS, Australia
Hygromycin B Gold (100 mg/mL)	InvivoGen, USA
Isotype PE-conjugated anti-mouse IgG antibody	Biolegend, USA
L-Glutamine	Thermo Fisher Scientific, USA

Chemicals and reagents	Origin
Lipofectamine 3000 reagents	InvivoGen, USA
Methylthiazolyldiphenyl-tetrazolium bromide (MTT)	Sigma-Merck KGaA, Germany
Nuclease-free water	ITW reagents-AppliChem, Germany
Opti-MEM™ reduced serum medium	Thermo Fisher Scientific, USA
Paraformaldehyde (PFA)	Sigma-Merck KGaA, Germany
Penicillin-streptomycin (10,000 U/mL)	Thermo Fisher Scientific, USA
PE-conjugated anti-human CD184 antibody (clone 12G5)	Biolegend, USA
Poly-L-lysine solution (0.01%)	InvivoGen, USA
pTriEX 1.1 Hygro expression vector	Novagen-Merck KGaA Germany
Red safe nucleic acid staining solution (20,000 x)	iNtRON Biotechnology, Korea
RevertAid first-strand cDNA synthesis kit	Thermo Fisher Scientific, USA
Sodium azide (NaN ₃)	Sigma-Merck KGaA, Germany
Sodium chloride (NaCl)	KEMAUS, Australia
T4 DNA ligase (5 Weiss U/μL)	Thermo Fisher Scientific, USA
Tris(hydroxymethyl)aminomethane (Tris)	OmniPur-Merck KGaA, Germany
Trypsin-EDTA solution (0.25%)	InvivoGen, USA
Trypton	Himedia, India
Yeast extract	Himedia, India
1X Tris-acetate EDTA (TAE) buffer	Laboratory preparation

3.2. Methods

3.2.1. Tested compounds

Extracted compounds of *Stephania pierrei* (crebanine, dehydrocrebanine and methoxy-8-uvariopsine) were obtained from our laboratory. AMD3100 and clonidine.HCl was diluted in water as stock solutions at 1 mM.

3.2.2. Cell culture

Human embryonic kidney (HEK)-293T cell line and human breast adenocarcinoma cell line (MDA-MB-231) (ATCC, VA, USA) were grown in complete DMEM media (DMEM supplemented with 10% FBS, 1% penicillin-streptomycin and 1% L-glutamine) at 37°C and 5% CO₂ atmosphere. *Escherichia coli* (*E. coli*) strain DH5 α (DH5 α *E. coli*) cells (New England Biolabs, MA, USA) were grown in Lennox (or LB) media. LB media was prepared by Trypton 10 g/L, yeast extracts 5 g/L and NaCl 5 g/L. For LB agar, agar powder was added at a final concentration of 1.5%.

3.2.3. Construction of recombinant CXCR4 plasmids

The RNA extracted from the Jurkat cell (T cell line) was used as a template for 5 isotypes of CXCR4 (A, B, C, D and E) amplification. Complementary DNA sequences (cDNAs) were synthesized using the RevertAid First Strand cDNA Synthesis kit. Full-length CXCR4 coding sequences of 5 isotypes were amplified according to the polymerase chain reaction (PCR) using specific primers as shown in Table 5. The primers are designed specifically for each CXCR4 isotype which is introduced *EcoRI* and *XhoI* restriction sites at the 5' ends of forward and reverse primers, respectively.

Table 5. Sequences of designed CXCR4 primers

Primers	Sequences
CXCR4-a Forward	5' <u>GAA TTC</u> TAT GTC CAT TCC TTT GCC TCT
CXCR4-b Forward	5' <u>GAA TTC</u> TAT GGA GGG GAT CAG TAT ATA
CXCR4-c/d Forward	5' <u>GAA TTC</u> TAT GGA GGG GAT CAG TGA AAA
CXCR4-e Forward	5' <u>GAA TTC</u> TAT GGG CTC AGG GGA CTA TGA
CXCR4 Reverse	5' <u>CTC GAG</u> TTA GCT GGA GTG AAA ACT TG

The CXCR4-A, -B, -C, -D, and -E amplicons were molecularly ligated into a cloning vector, pJET1.2/blunt vector according to the manufacturer's instruction. Then, they were subsequently subcloned into pTriEXTM-1.1 Hygro expression vector. The pTriEXTM-1.1 Hygro plasmid and CXCR4-A, -B, -C, -D, and -E-pJET1.2/blunt

plasmids were digested by *EcoRI* and *XhoI* restriction enzymes. Gel electrophoresis is performed to determine the efficiency of enzyme digestion. The agarose gels containing the linear pTriEX™-1.1 Hygro plasmid and CXCR4-A, -B, -C, -D, and -E coding sequences were excised and purified by GenHlow™ Gel/PCR kit. Finally, the purified digested CXCR4-A, -B, -C, -D, and -E fragments were molecularly ligated to the linear pTriEX™-1.1 Hygro plasmid using a T4 DNA ligation kit. The ligations were transfected into competent DH5α *E. coli* cells by the heat-shock method. Transformed DH5α *E. coli* were spread on the LB agar supplemented with 100 µg/mL of ampicillin (LB-A) agar plate and incubated at 37°C for 16-18 hrs. The DH5α *E. coli* colonies on LB-A agar were randomly screened by colony PCR using universal plasmid-specific primers (T7 promoter and IRES reverse primers). Table 6 displayed colony PCR master mix preparation, and Table 7 presented the conditions set up for colony PCR reaction. The PCR product was visualized on 1% agarose gel by gel electrophoresis.

Table 6. Master mix preparation for colony PCR

PCR master mix component	Volume (µL)
Taq buffer	1.25
2 mM MgCl ₂	0.75
dNTP	0.5
Primer forward	0.25
Primer reverse	0.25
Taq DNA polymerase	0.1
Nuclease-free water	9.4
Total volume	12.5

Table 7. Conditions for the colony PCR reaction

PCR steps	Temperature	Time	Cycle
Initial denaturation	95°C	10 min	1
Denaturation	95°C	30 sec	
Annealing	55°C	30 sec	30
Extension	72°C	1:15 min	
Final extension	72°C	10 min	1
End	10°C	Pause	

The recombinant CXCR4-A, -B, -C, -D, and -E-pTriEX™ 1.1 Hygro plasmids were extracted by the Favorprep kit. Briefly, the DH5α *E. coli* transformants carrying CXCR4-A, -B, -C, -D, and -E-pTriEX™ 1.1 Hygro plasmids were cultured individually in LB media supplemented with 100 µg/mL of ampicillin at 37°C, 250 rpm-shaking for 16-18 hrs. After pelleting, the CXCR4-A, -B, -C, -D, and -E - pTriEX™ 1.1 Hygro plasmids were extracted following the manufacturer's instruction and quantified the concentration by Nanodrop 8000 UV-Vis spectrophotometer (Thermo Scientific). The CXCR4-pTriEX™ 1.1 Hygro plasmids were sequenced and analyzed by CLC Main Workbench 20 (Qiagen Digital Insights). The amino acid sequences of all CXCR4 isotypes were deduced and aligned with CXCR4 sequences in the databases by Basic Local Alignment Search Tool (BLAST) programs supported by the National Center of Biotechnology Information (NCBI) website and Clustal Omega program.

3.2.4. Generation of stable CXCR4-overexpressed cell line

3.2.4.1. Hygromycin B kill curve/titration

The HEK293T cells were transfected with CXCR4-pTriEX™ 1.1 Hygro plasmids harboring the hygromycin resistance (*hph*) gene. Thus, the cells can be selected with hygromycin B to obtain stable cell lines. Briefly, hygromycin B titration was performed to determine the optimal antibiotic dose for selecting the stable cell

colonies. The experiment was based on hygromycin B quick reference protocol (MirusBio, US). In particular, normal HEK293T cells were seeded in a 96-well plate (10^4 cells in 0.1 mL complete DMEM media per well) and incubated at 37°C and 5% CO₂ condition for 1 day. When the cell confluence reached $\geq 80\%$, various concentrations of hygromycin (0, 150, 200, 250, 500, 600, 700 and 800 $\mu\text{g/mL}$) were added to the HEK293T cells and incubated for 7 days. The cell cultures were examined every day under microscopy for visual toxicity, while the selective media were replaced every 2-3 days up to a week. After 7 days of selection, the lowest concentration of antibiotic at which all cells were dead was considered as the optimal dose. Moreover, the high dose was the concentration of antibiotic at which cells were killed within the first 2-3 days of selection. The low dose was the antibiotic concentration at which minimal toxicity was observed after 7 days.

3.2.4.2. Stable transfection of CXCR4-pTriEX™ 1.1 Hygro plasmids in HEK293T

Normal HEK293T cells were seeded in a 24-well plate (1.5×10^5 cells in 0.5 mL complete DMEM media per well) for 1 day to reach confluency around 70-90% before stable transfection. HEK293T cells were transfected respectively with 0.5 μg , 1 μg and 1.5 μg of CXCR4-pTriEX™-1.1 Hygro plasmids using lipofectamine 3000 reagents for 2 days. One well was used as a negative control. After 2 days of incubation, both transfected and normal cells were treated with hygromycin B at the optimal concentration as described in 3.2.4.1. The cell cultures were examined every day under microscopy for the signs of visual toxicity. Distinct colonies of surviving cells that appeared in the transfected cell cultures were considered as the colonies of stably transfected cells with recombinant CXCR4 (or rCXCR4) plasmids. In contrast, normal cells were killed entirely in the negative control. The fresh complete DMEM supplemented with an optimal concentration of hygromycin B was replaced every 3-5 days to remove dead cells and debris. After transfected HEK293T cells reached 90-100% confluence, the rCXCR4 expression was determined by flow cytometry.

3.2.5. Isolation of CXCR4-overexpressed HEK293T

For stably highly CXCR4 expressed HEK293T cells isolation, the rCXCR4-expressed HEK293T cells (2×10^6 cells) were collected and washed with the filtered sorting buffer (2% FBS in PBS). The rCXCR4-expressed HEK293T cells were blocked with 20% FBS in sorting buffer and incubated on ice for 30 minutes (min). After washing, the rCXCR4-HEK293T cells were stained with phycoerythrin (PE)-conjugated anti-human CD184 (anti-hCD184) antibody for 30 min on ice. Then, the transfected cells were washed and filtered using the sorting tubes with filter caps. The rCXCR4 expressed HEK293T cells were detected and sorted by fluorescence-activated cell sorting (FACS) flow cytometer. Finally, the sorting cells were washed with complete DMEM and incubated at 37°C, 5% CO₂.

3.2.6. Freezing cell stock and mycoplasma contamination test

After the stable CXCR4-transfected HEK293T and isolated CXCR4-overexpressed HEK293T cells expanded in the T75 flask at the high confluence (90-100% confluence), they were detached by 0.25% trypsin-EDTA and washed with PBS, pH 7.4 (~10 mL) twice by centrifuging at speed 150 x g and 25°C for 5 min. Cell pellets were re-suspended in the freezing media containing 90% FBS and 10% DMSO and divided into each cryovial at concentration 1-1.5 x 10⁶ cells/mL to freeze as the cell stocks. The cryovials were kept in a freezer at temperature -80°C before storing in a liquid nitrogen tank.

The contamination of mycoplasma (MP) bacteria in the cell cultures was tested by PCR technique. Briefly, cell cultures of CXCR4-transfected HEK293T cells were collected in microcentrifuge tubes (~500 µL) and boiled for 5 min. The air pressure in the tubes should be released every 10-20 seconds [48]. Sample tubes were centrifuged at 10,000 x g, and the sample supernatants were used for PCR. Table 8 and Table 9 displayed PCR master mix preparation and the conditions set up for mycoplasma contamination test, respectively. The test is based on detecting the 16S rRNA gene of Mycoplasma species commonly found in contaminated cell cultures [65]. It is an essential step to keep our cells are homogenous and protect the DNA sequence of cells from the changes caused by mycoplasma.

Table 8. PCR master mix preparation for mycoplasma contamination test

PCR master mix component	Volume (μL)
Taq buffer	1.25
2 mM MgCl_2	0.75
dNTP	0.5
Primer forward (specific for MP)	0.25
Primer reverse (specific for MP)	0.25
Taq DNA polymerase	0.1
Nuclease-free water	7.4
Total volume	10.5

Table 9. PCR condition for mycoplasma contamination test

PCR steps	Temperature	Time	Cycle
Initial denaturation	95°C	30 sec	1
Denaturation	95°C	10 sec	
Annealing	55°C	30 sec	34
Extension	68°C	35 sec	
Final extension	68°C	5 min	1
End	4°C	Pause	

3.2.7. Investigation of CXCR4 expression in HEK293T cells

The CXCR4-transfected HEK293T cells, the CXCR4-overexpressed HEK293T cells, and the isolated cells after cell sorting described in 3.2.4 were investigated for expression level. The CXCR4-transfected HEK293T cells were first detached by 0.25% trypsin-EDTA and washed with PBS, pH 7.4. They were prepared in microcentrifuge tubes ($1-2 \times 10^5$ cells) and centrifuged at speed $10,000 \times g$ for 1

minute by microcentrifuge (Eppendorf-5417C). The supernatant was discarded, while the cell pellet was washed with PBS (500 μ L) and centrifuged at 10,000 x g for 1 minute. For blocking the binding of antibodies with the fragment crystallizable (Fc) receptors on cells and reducing of fluorescent background, the cell pellet was then incubated with 50 μ L of 10% human AB serum in FACS buffer for 30 min and stained with 2.5 μ L of PE-conjugated anti-hCD184 antibody (1:200) on ice for 30 min in dark. After washing, the transfected cells were fixed with 500 μ L of 1% paraformaldehyde (PFA) in FACS buffer in 5 mL-polystyrene ground-bottom tubes and detected signal by FACSCalibur flow cytometer (Becton Dickinson Biosciences, US). The HEK293T cells were parallelly stained as the background control.

3.2.8. Verification of CXCR4-overexpressed HEK293T cells

3.2.8.1. Saturation binding assay of PE-conjugated anti-hCD184 antibody

To perform this experiment, 1×10^5 of CXCR4 highly expressing HEK293T cells and normal HEK293T cells were seeded onto a poly-L-lysine pre-treated 96-well black plate and incubated at 37°C, 5% CO₂ atmosphere 16-18 hrs. The monolayers of both cells were washed with PBS, pH 7.4 and fixed with 4% paraformaldehyde in PBS for 20 min at room temperature. Then, the cells were blocked with 5% BSA in PBS at room temperature for 30 min. After washing, the cells were incubated with various concentrations of PE-conjugated anti-CXCR4 antibody (1, 5, 10, 50, 100, 250, 500, 1000, 5000, 10000 and 20000 pM) at room temperature in dark for 1 hour. The cells treated with only PBS were considered as negative controls. After washing, the fluorescent signal was detected at excitation and emission wavelengths of 550 and 578 nm, respectively, using spectrophotometric microplate reader Synergy™ H1 (BioTek-Agilent, USA). The half-maximal effective concentration (EC₅₀) of anti-hCD184 antibody was calculated using GraphPad Prism 9 (GraphPad Software Inc., CA, USA).

3.2.8.2. Competitive binding assay of CXCR4 antagonist (AMD3100)

To perform a competitive binding assay, the CXCR4 highly expressing HEK293T cells and normal HEK293T cells (1×10^5 cells/well) were seeded separately onto a poly-L-lysine pre-treated 96 well black plates and incubated at 37°C, 5% CO₂

atmosphere for 16-18 hrs. After washing with PBS, the monolayer cells were fixed with 4% PFA in PBS at room temperature for 20 min, followed by blocking with 5% BSA in PBS for 30 min at room temperature. Six serial concentrations of AMD3100 (0.5, 5, 50, 500, 5000 and 50000 nM) were added to the designed wells (Figure 7) and incubated for 30 min at room temperature. The cells treated with only PBS were considered as a negative control. After washing, the monolayer cells were incubated with a fixed concentration of PE-conjugated anti-hCD184 antibody for 30 min in dark at room temperature. The fixed concentration of antibodies was given from the saturation binding assay. The fluorescent signal was determined as described above. The half-maximal inhibitory concentration (IC_{50}) of the AMD3100 was analyzed by GraphPad Prism 9.

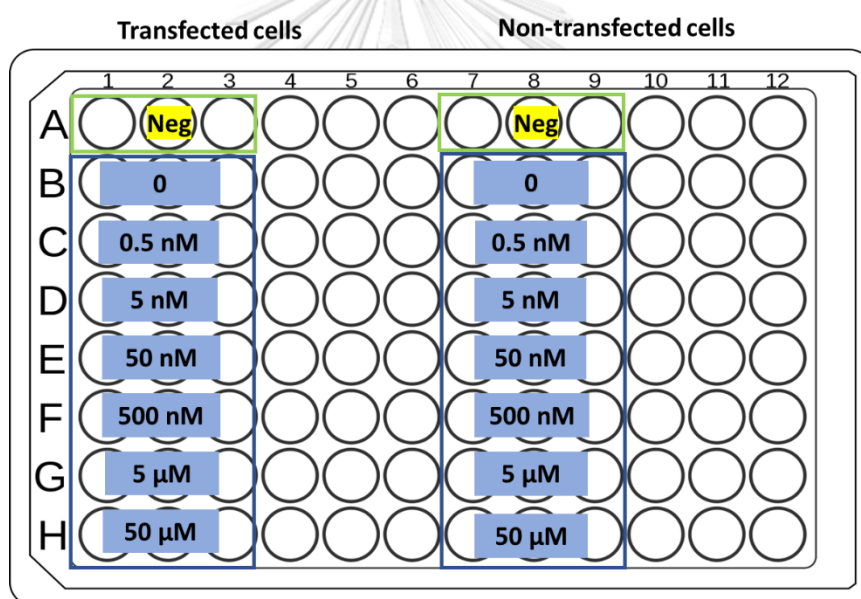


Figure 7. The designed 96-well plate for competitive binding assay of AMD3100

3.2.9. Determination of binding affinity of natural compounds to CXCR4

3.2.9.1. Cytotoxicity assay of natural compounds in cancer cell lines

MDA-MB-231 cells were seeded into 96-well plates at a density of 20,000 cells/well in 200 μ L of complete DMEM media cultured for 24 hrs at 37°C in a 5% CO_2 atmosphere. Natural compounds (crebanine, dehydrocrebanine and methoxy-8-uvариopsine) were dissolved in DMSO and diluted with serum-free media to obtain

the final concentrations at 1, 10, 20, 50 and 100 μM . Complete media containing 0.5% DMSO served as the negative controls. Cells were then treated with natural compounds at indicated concentrations. After 1 day of incubation, the media was removed, and the cells were washed twice with phosphate-buffered saline (PBS, pH 7.4). Cell viability was evaluated using the MTT assay. MTT solution (1 mg/mL in serum-free media) was added into cell culture (200 μL per well) and incubated in the dark for 3 hrs. The MTT solution was removed, and 200 μL DMSO was added to each well to solubilize formazan crystals. The absorbance of the formazan solution was measured at a wavelength of 570 nm using a microplate reader. The experiment was performed with three replicates for each treatment. The half-maximal inhibitory concentration (IC_{50}) values of the natural compounds were determined based on the percentage of cell viability.

3.2.9.2. Competitive binding assay of natural compounds

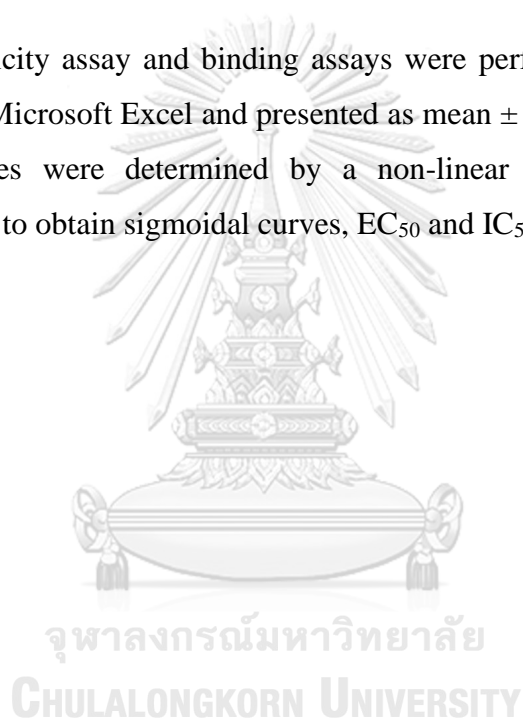
Similar to the competitive binding assay of AMD3100, the CXCR4 highly expressing HEK293T cells and normal HEK293T cells (1×10^5 cells/well) were seeded separately onto a poly-L-lysine pre-treated 96 well black plates and incubated at 37°C , 5% CO_2 atmosphere for 16-18 hrs. After washing with PBS, the monolayer cells were fixed with 4% PFA in PBS at room temperature for 20 min, followed by blocking with 5% BSA in PBS for 30 min at room temperature. Various concentrations of natural compounds were added to the indicated wells (as designed in Table 10) and incubated for 30 min at room temperature. The cells treated with only PBS were considered as the first negative control. In addition, clonidine hydrochloride and AMD3100 were used as the second negative control and positive control, respectively. After washing, the monolayer cells were incubated with a fixed concentration of PE-conjugated anti-hCD184 antibody for 30 min in dark at room temperature. The fluorescent signal was determined at excitation and emission wavelengths of 550 and 578 nm, respectively, using spectrophotometric microplate reader SynergyTM H1 (BioTek-Agilent, USA). The half-maximal inhibitory concentration (IC_{50}) of the natural compounds was analyzed by GraphPad Prism 9.

Table 10. The concentrations of natural compounds in different trials

Trial	Concentrations	Vehicle
1	0.5 nM, 5 nM, 50 nM, 500 nM, 5 μ M and 50 μ M	0.5% DMSO/PBS
2	1 μ M, 10 μ M, 50 μ M, 100 μ M, 200 μ M and 400 μ M	100% DMSO
3	1 μ M, 10 μ M, 50 μ M, 100 μ M and 200 μ M	0.5% DMSO+0.5% Tween 20

3.2.10. Statistical analysis

The cytotoxicity assay and binding assays were performed in triplicates. Data were analyzed in Microsoft Excel and presented as mean \pm SD. For the binding assay, the binding curves were determined by a non-linear regression method using GraphPad Prism 9 to obtain sigmoidal curves, EC₅₀ and IC₅₀ values.



CHAPTER 4. RESULTS AND DISCUSSION

4.1. Production of CXCR4-overexpressed HEK293T cells

The process of producing the transfected HEK293T cells stably overexpressing CXCR4 for competitive binding assay of natural compounds targeting CXCR4 was described as in Figure 8.

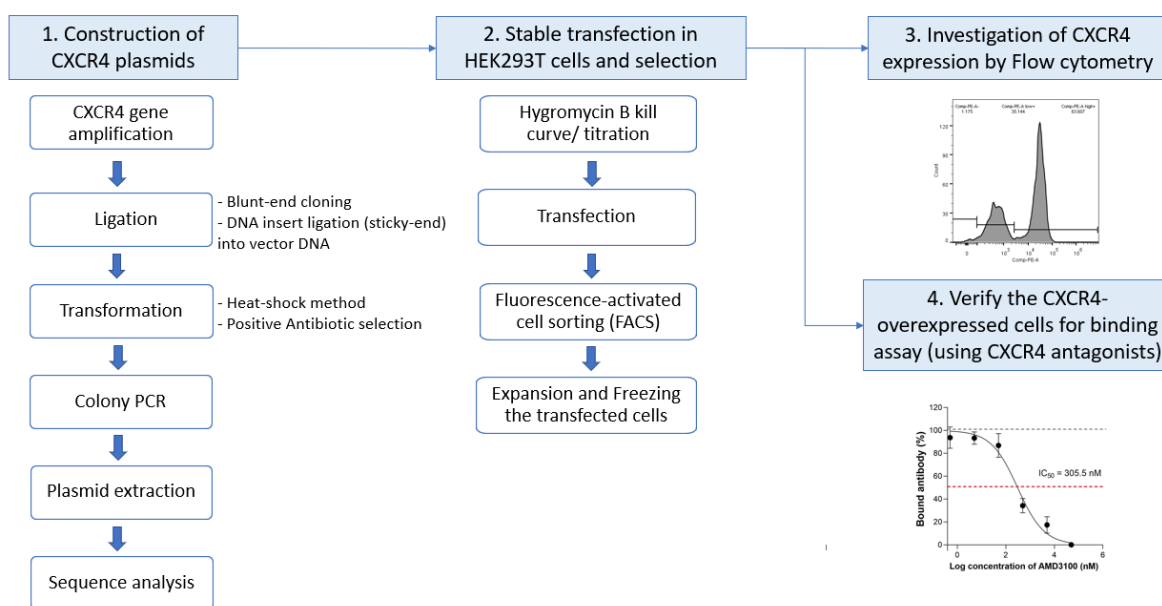


Figure 8. Production of transfected HEK293T cells stably expressing recombinant CXCR4 for binding assay

4.1.1. Recombinant CXCR4 plasmids construction

A total of five different full-length CXCR4-coding sequences, namely isotypes A, B, C, D and E, were amplified by PCR. These blunt-end PCR products were verified by 1% agarose gel electrophoresis. The sizes of CXCR4 coding sequences were ~1000 base pairs (bp) (Figure 9). The PCR amplicons were ligated into pJET1.2/blunt cloning vectors and subsequently sub-cloned into pTriEX™-1.1 Hygro expression vectors (Figure 10). The recombinant CXCR4-A, -B, -C, -D, and -E plasmids carrying *E. coli* were randomly screened by PCR (Figure 11 and 14).

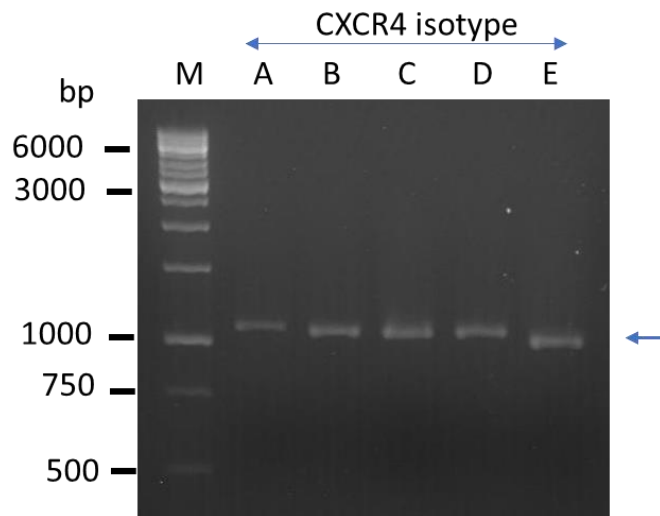


Figure 9. PCR amplicons of DNA sequences coding for 5 isotypes of CXCR4 (~1000 bp). Lane M: 1 kb DNA ladder marker; Lane A: CXCR4 isotype A amplicon; Lane B: CXCR4 isotype B amplicon; Lane C: CXCR4 isotype C amplicon; Lane D: CXCR4 isotype D amplicon; Lane E: CXCR4 isotype E amplicon. Numbers at the left are DNA sizes in bp.

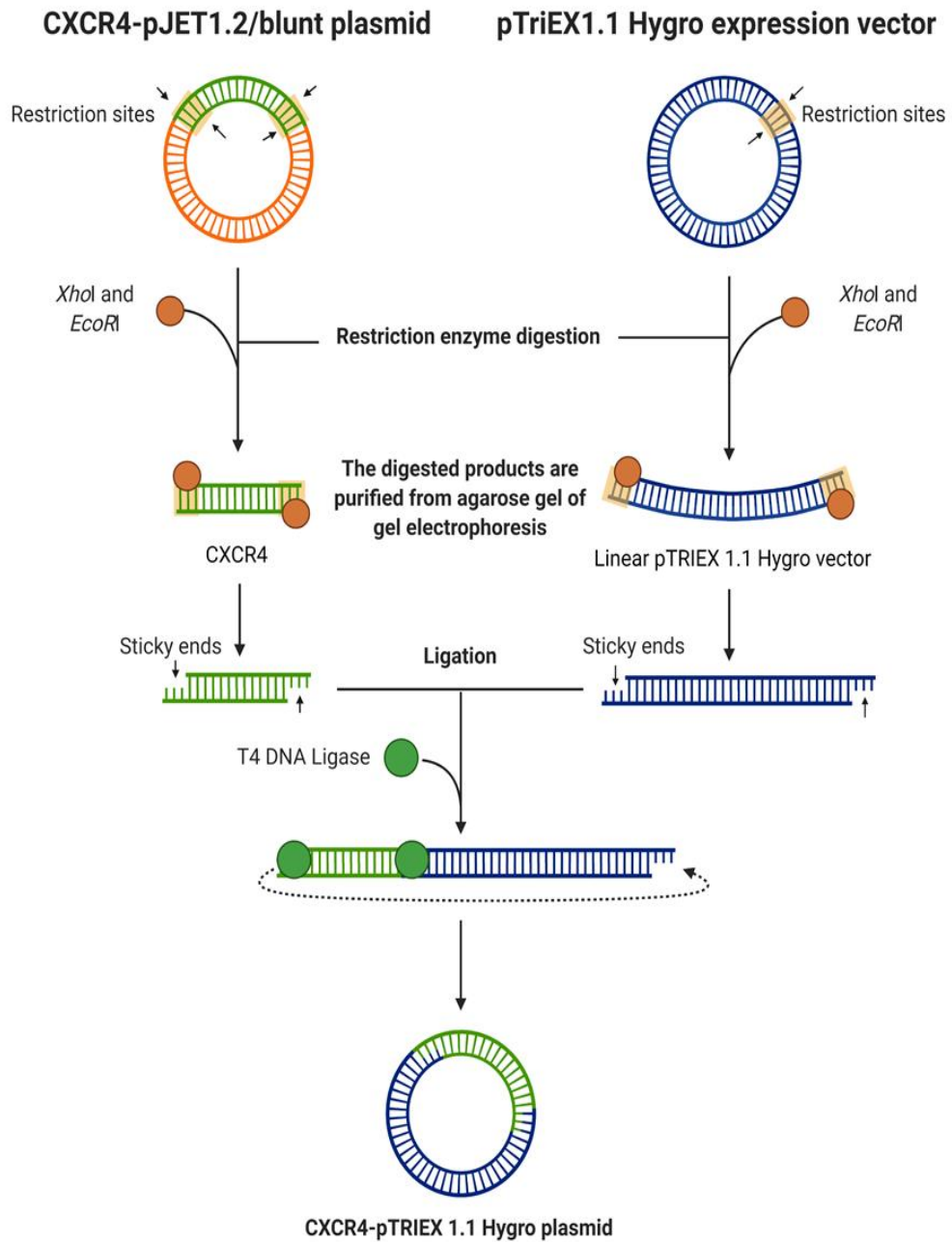


Figure 10. A flow diagram of the CXCR4 cloning procedure

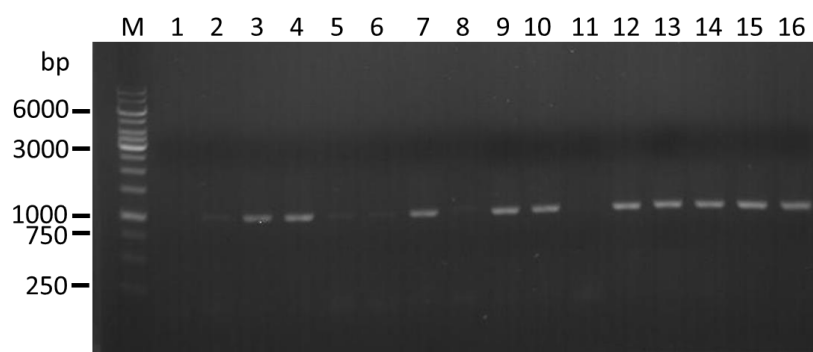


Figure 11. Representatives of PCR amplicons of DNA sequences coding for CXCR4 (~1000 bp) from the CXCR4-pJET1.2/blunt plasmids. Lane M: 1 kb DNA ladder marker; Lane 1: Negative control; Lane 2-16: CXCR4 amplicons from *E. coli* clone 1-15, respectively. Numbers at the left are DNA sizes in bp

Table 11. Positive results of the transformation of CXCR4 isotypes with pJET1.2/blunt vectors into *E. coli* DH5 α cells using colony PCR technique

CXCR4 isotype	Number of positive colonies	Inoculated clones
A	5	A9, A11
B	5	B6, B13
C	6	C1, C2
D	6	D1, D2
E	10	E11, E12

To subclone CXCR4 genes into expression vectors, pTriEXTM-1.1 Hygro vectors and CXCR4 fragments from extracted CXCR4-pJET1.2/blunt plasmids were used and cut by restriction enzymes *Xho*I and *Eco*RI (Figure 12 and 13). Total 8 clones of the CXCR4 isotype were successfully digested by enzymes, including A9, A11, B6, C2, D1, D2, E11 and E12. However, only 5 clones (A9, B6, C2, D1, D2 and E12) were applied for ligation with linear pTriEXTM1.1 Hygro vector to construct CXCR4-pTriExTM1.1 Hygro plasmids and transformation with *E. coli* DH5 α cells. Similar to the construction of CXCR4-pJET1.2/blunt plasmids, positive colonies carrying CXCR4-pTriEXTM1.1 Hygro plasmid were selected in LB/Amp agar plate and detected by colony PCR technique.

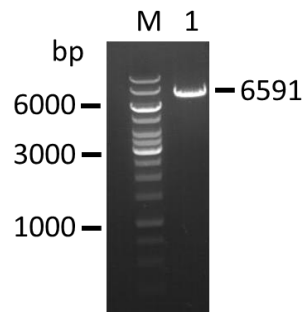


Figure 12. The agarose gel of pTriEX™ 1.1 Hygro vectors after enzyme digestion reaction. Lane M: 1 kb DNA ladder marker; Lane 1: digested pTriEX™ 1.1 Hygro vectors. Numbers at the left are DNA sizes in bp

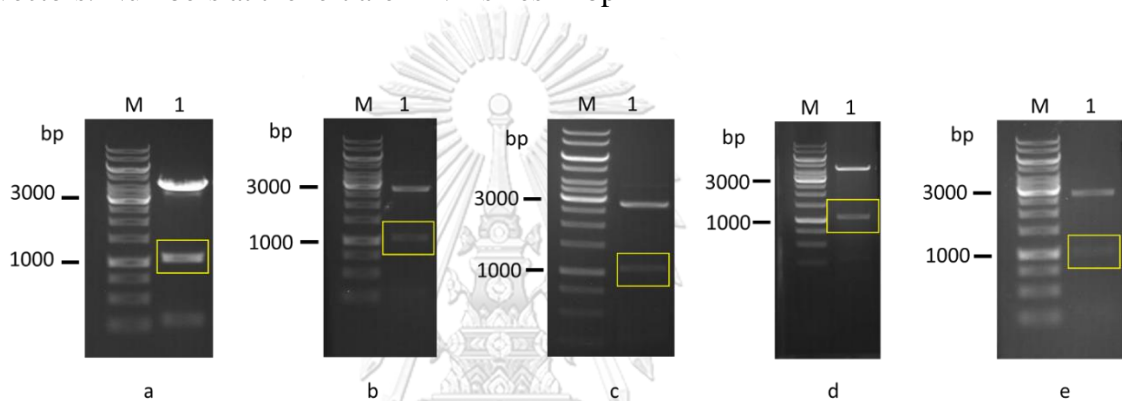


Figure 13. The agarose gel of CXCR4-pJET1.2/blunt plasmids after digestion reaction with *XhoI* and *EcoRI* restriction enzymes. Lane M: 1 kb DNA ladder marker; Lane 1: digested products of CXCR4-pJET1.2/blunt plasmids of isotypes (a) A9; (b) B6; (c) C2 (d) D1 and (e) E12, respectively, which contain the band of CXCR4 (~1000 bp)

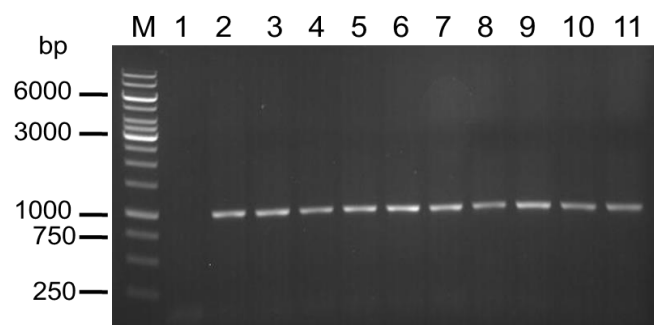


Figure 14. Representatives of PCR amplicons of DNA sequences coding for CXCR4 (~1000 bp) from the CXCR4-pTriEX™ 1.1 Hygro plasmids. Lane M: 1 kb DNA ladder marker; Lane 1: Negative control; Lane 2-11: CXCR4 amplicons from *E. coli* clones 1-10, respectively. Numbers at the left are DNA sizes in bp.

Concentrations of extracted CXCR4-pJET1.2/blunt and CXCR4-pTriEX™ 1.1 Hygro plasmids were determined by Nanodrop 8000 UV-Vis spectrophotometer and presented in Table 12.

Table 12. The concentration of extracted recombinant CXCR4 plasmids

rCXCR4 plasmid	Concentration (ng/μL)	rCXCR4 plasmid	Concentration (ng/μL)
A9-pJET1.2/blunt	851.1	A9.1-pTriEX1.1™ Hygro	462.6
A11-pJET1.2/blunt	495.8	A9.2-pTriEX1.1™ Hygro	455.2
B6-pJET1.2/blunt	192.0	B6.1-pTriEX1.1™ Hygro	369.0
B13-pJET1.2/blunt	419.0	B6.2-pTriEX1.1™ Hygro	483.4
C1-pJET1.2/blunt	243.7	C2.1-pTriEX1.1™ Hygro	268.2
C2-pJET1.2/blunt	162.8	C2.2-pTriEX1.1™ Hygro	330.1
D1-pJET1.2/blunt	162.8	D1.1-pTriEX1.1™ Hygro	557.1
D2-pJET1.2/blunt	69.3	D1.2-pTriEX1.1™ Hygro	447.7
E11-pJET1.2/blunt	125.5	D2.1-pTriEX1.1™ Hygro	523.9
E12-pJET1.2/blunt	65.8	D2.2-pTriEX1.1™ Hygro	597.6
-	-	E12.1-pTriEX1.1™ Hygro	827.2
-	-	E12.2-pTriEX1.1™ Hygro	1005.0

The CXCR4-A, -B, -C, -D, and -E-pTriEX™-1.1 Hygro plasmids were sequenced, analyzed, deduced, and blasted with the database. The result showed that CXCR4-coding sequences of isotype A, B and E were similar to the reference human CXCR4-coding sequences on the NCBI database, except isotype C and D (Table 13, Figure 15 and Figure A1-3). However, the DNA sequences of CXCR4-C and CXCR4-D were similar to the sequence of CXCR4-isotype B based on the BLAST results (Figure A4-5). According to the proteins sequence alignment results, the sequences of CXCR4-C and CXCR4-D have also been found different from reference

protein sequences of isotype C and D on the database. No mutation was found in all CXCR4 isotypes in the constructed CXCR4 plasmids (Table 14 and Figure 16).

Table 13. Information of reference CXCR4 DNA sequences

CXCR4 isotype	Database
A	Homo sapiens C-X-C motif chemokine receptor 4 (CXCR4), transcript variant 1. NCBI_ID: NM_001008540.2
B	Homo sapiens C-X-C motif chemokine receptor 4 (CXCR4), transcript variant 2. NCBI_ID: NM_003467.3
C	Homo sapiens C-X-C motif chemokine receptor 4 (CXCR4), transcript variant 3. NCBI_ID: NM_001348056.2
D	Homo sapiens C-X-C motif chemokine receptor 4 (CXCR4), transcript variant 4. NCBI_ID: NM_001348059.2
E	Homo sapiens C-X-C motif chemokine receptor 4 (CXCR4), transcript variant 5. NCBI_ID: NM_001348060.2

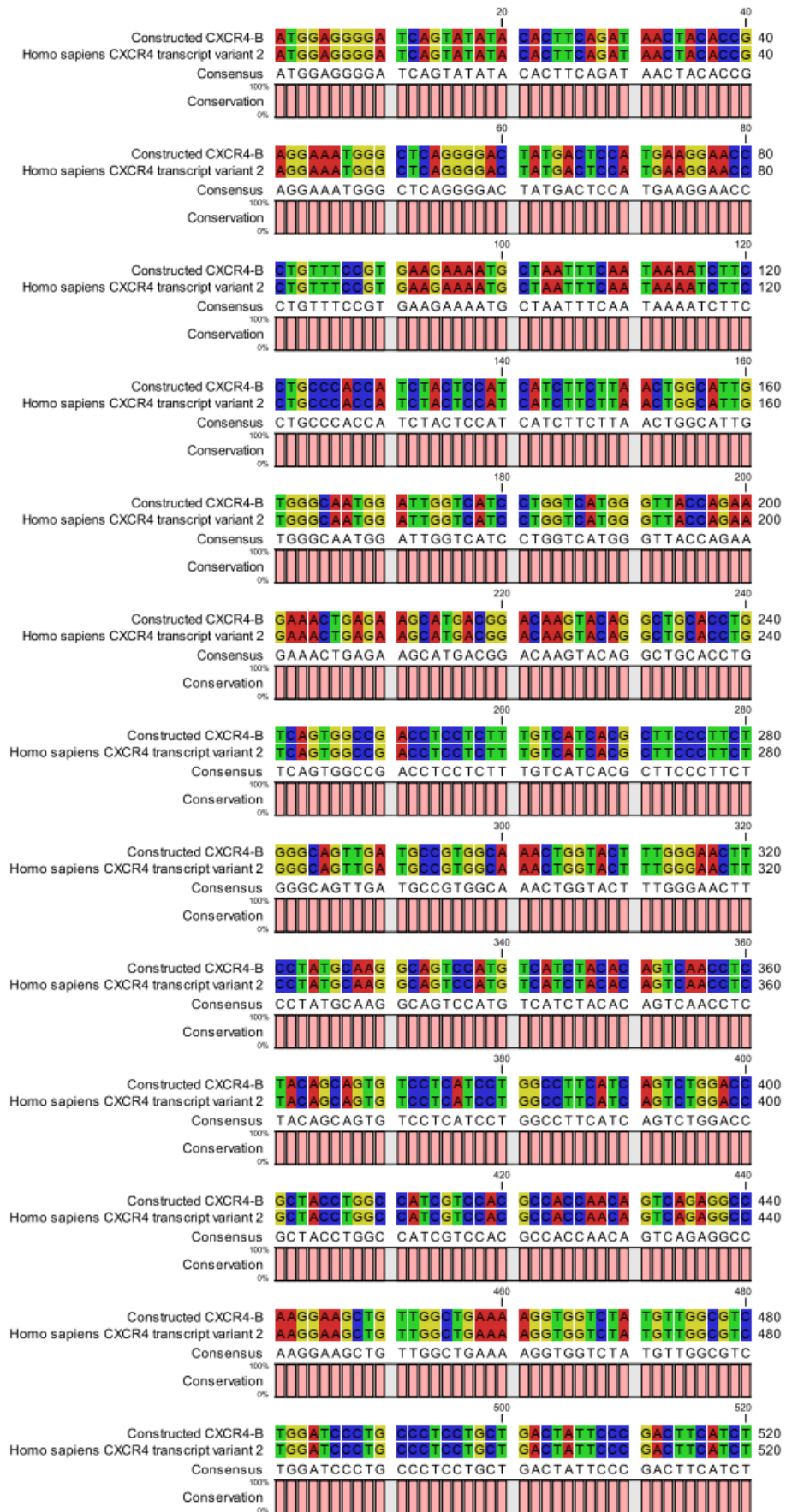




Figure 15. The representative alignment results of constructed CXCR4-B DNA sequence with reference DNA sequence (Homo sapiens CXCR4 transcript variant 2_ NM_003467.3) on NCBI database.

Table 14. Information of reference CXCR4 protein sequences

Reference protein sequence	Length (aa)	NCBI_ID
CXCR4-A	356	NP_001008540.1
CXCR4-B	352	NP_003458.1
CXCR4-C	423	NP_001334985.1
CXCR4-D	385	NP_001334988.1
CXCR4-E	337	NP_001334989.1

CLUSTAL O(1.2.4) multiple sequence alignment

N-terminal segment				
Ref. CXCR4-B	-----	0		
CXCR4-B	-----	0		
CXCR4-C	-----	0		
CXCR4-D	-----	0		
Ref. CXCR4-D	MEGISENAPLPNVPNAPSDKHEDGKRPHRRSARLGEE-----	38		
Ref. CXCR4-C	MEGISENAPLPNVPNAPSDKHEDGKRPHRRSARLGEEVFPVHFLTLPPNIPQAPKGLRF	60		
Ref. CXCR4-A	-----	0		
CXCR4-A	-----	0		
Ref. CXCR4-E	-----	0		
CXCR4-E	-----	0		
N-terminal segment		TM1		
Ref. CXCR4-B	-----MEGISIYTSDNYTEEMGSGDYDSMKEPCFREANANFNK	IFLPTIYSIIF 49		
CXCR4-B	-----MEGISIYTSDNYTEEMGSGDYDSMKEPCFREANANFNK	IFLPTIYSIIF 49		
CXCR4-C	-----MEGISIYTSDNYTEEMGSGDYDSMKEPCFREANANFNK	IFLPTIYSIIF 49		
CXCR4-D	-----MEGISIYTSDNYTEEMGSGDYDSMKEPCFREANANFNK	IFLPTIYSIIF 49		
Ref. CXCR4-D	-----IYTSDNYTEEMGSGDYDSMKEPCFREANANFNK	IFLPTIYSIIF 82		
Ref. CXCR4-C	KTAFSLPTTSCLKPRMIYTSDNYTEEMGSGDYDSMKEPCFREANANFNK	IFLPTIYSIIF 120		
Ref. CXCR4-A	-----MSIPLPLLQIYTSDNYTEEMGSGDYDSMKEPCFREANANFNK	IFLPTIYSIIF 53		
CXCR4-A	-----MSIPLPLLQIYTSDNYTEEMGSGDYDSMKEPCFREANANFNK	IFLPTIYSIIF 53		
Ref. CXCR4-E	-----MGS GDYDSMKEPCFREANANFNK	IFLPTIYSIIF 34		
CXCR4-E	-----MGS GDYDSMKEPCFREANANFNK	IFLPTIYSIIF 34		
	*****	*****		
TM1	ICL1	TM2	ECL1	
Ref. CXCR4-B	LTGIVGNGLVILVM	GYQKKLRSMTDKYR	LHLSVADLLFVITLPPFWAVDAV	ANWYFGNFLC 109
CXCR4-B	LTGIVGNGLVILVM	GYQKKLRSMTDKYR	LHLSVADLLFVITLPPFWAVDAV	ANWYFGNFLC 109
CXCR4-C	LTGIVGNGLVILVM	GYQKKLRSMTDKYR	LHLSVADLLFVITLPPFWAVDAV	ANWYFGNFLC 109
CXCR4-D	LTGIVGNGLVILVM	GYQKKLRSMTDKYR	LHLSVADLLFVITLPPFWAVDAV	ANWYFGNFLC 109
Ref. CXCR4-D	LTGIVGNGLVILVM	GYQKKLRSMTDKYR	LHLSVADLLFVITLPPFWAVDAV	ANWYFGNFLC 142
Ref. CXCR4-C	LTGIVGNGLVILVM	GYQKKLRSMTDKYR	LHLSVADLLFVITLPPFWAVDAV	ANWYFGNFLC 180
Ref. CXCR4-A	LTGIVGNGLVILVM	GYQKKLRSMTDKYR	LHLSVADLLFVITLPPFWAVDAV	ANWYFGNFLC 113
CXCR4-A	LTGIVGNGLVILVM	GYQKKLRSMTDKYR	LHLSVADLLFVITLPPFWAVDAV	ANWYFGNFLC 113
Ref. CXCR4-E	LTGIVGNGLVILVM	GYQKKLRSMTDKYR	LHLSVADLLFVITLPPFWAVDAV	ANWYFGNFLC 94
CXCR4-E	LTGIVGNGLVILVM	GYQKKLRSMTDKYR	LHLSVADLLFVITLPPFWAVDAV	ANWYFGNFLC 94
	*****	*****	*****	*****
TM3	ICL2	TM4		
Ref. CXCR4-B	K AVHVIYTVNLYSSVLILAFI	SLDRYLAIIVHATNSQRPRKLLAEK	VVYVGVWIPALLLTI 169	
CXCR4-B	K AVHVIYTVNLYSSVLILAFI	SLDRYLAIIVHATNSQRPRKLLAEK	VVYVGVWIPALLLTI 169	
CXCR4-C	K AVHVIYTVNLYSSVLILAFI	SLDRYLAIIVHATNSQRPRKLLAEK	VVYVGVWIPALLLTI 169	
CXCR4-D	K AVHVIYTVNLYSSVLILAFI	SLDRYLAIIVHATNSQRPRKLLAEK	VVYVGVWIPALLLTI 169	
Ref. CXCR4-D	K AVHVIYTVNLYSSVLILAFI	SLDRYLAIIVHATNSQRPRKLLAEK	VVYVGVWIPALLLTI 202	
Ref. CXCR4-C	K AVHVIYTVNLYSSVLILAFI	SLDRYLAIIVHATNSQRPRKLLAEK	VVYVGVWIPALLLTI 240	
Ref. CXCR4-A	K AVHVIYTVNLYSSVLILAFI	SLDRYLAIIVHATNSQRPRKLLAEK	VVYVGVWIPALLLTI 173	
CXCR4-A	K AVHVIYTVNLYSSVLILAFI	SLDRYLAIIVHATNSQRPRKLLAEK	VVYVGVWIPALLLTI 173	
Ref. CXCR4-E	K AVHVIYTVNLYSSVLILAFI	SLDRYLAIIVHATNSQRPRKLLAEK	VVYVGVWIPALLLTI 154	
CXCR4-E	K AVHVIYTVNLYSSVLILAFI	SLDRYLAIIVHATNSQRPRKLLAEK	VVYVGVWIPALLLTI 154	
	*****	*****	*****	
TM4	ECL2	TM5	ICL3	
Ref. CXCR4-B	PDFIF ANVSEADDRYICDRFYPNDLW	VVVFQFQHIMVGLILPGIVIL	SCYCIIISKLSHS	229
CXCR4-B	PDFIF ANVSEADDRYICDRFYPNDLW	VVVFQFQHIMVGLILPGIVIL	SCYCIIISKLSHS	229
CXCR4-C	PDFIF ANVSEADDRYICDRFYPNDLW	VVVFQFQHIMVGLILPGIVIL	SCYCIIISKLSHS	229
CXCR4-D	PDFIF ANVSEADDRYICDRFYPNDLW	VVVFQFQHIMVGLILPGIVIL	SCYCIIISKLSHS	229
Ref. CXCR4-D	PDFIF ANVSEADDRYICDRFYPNDLW	VVVFQFQHIMVGLILPGIVIL	SCYCIIISKLSHS	262
Ref. CXCR4-C	PDFIF ANVSEADDRYICDRFYPNDLW	VVVFQFQHIMVGLILPGIVIL	SCYCIIISKLSHS	300
Ref. CXCR4-A	PDFIF ANVSEADDRYICDRFYPNDLW	VVVFQFQHIMVGLILPGIVIL	SCYCIIISKLSHS	233
CXCR4-A	PDFIF ANVSEADDRYICDRFYPNDLW	VVVFQFQHIMVGLILPGIVIL	SCYCIIISKLSHS	233
Ref. CXCR4-E	PDFIF ANVSEADDRYICDRFYPNDLW	VVVFQFQHIMVGLILPGIVIL	SCYCIIISKLSHS	214
CXCR4-E	PDFIF ANVSEADDRYICDRFYPNDLW	VVVFQFQHIMVGLILPGIVIL	SCYCIIISKLSHS	214
	*****	*****	*****	*****
ICL3	TM6	ECL3	TM7	
Ref. CXCR4-B	KGHQKRKALKTT VILILAFFACWLPYYIGISI	DSFILLEI IKQGEFENTVHK	WISITEA	289
CXCR4-B	KGHQKRKALKTT VILILAFFACWLPYYIGISI	DSFILLEI IKQGEFENTVHK	WISITEA	289
CXCR4-C	KGHQKRKALKTT VILILAFFACWLPYYIGISI	DSFILLEI IKQGEFENTVHK	WISITEA	289
CXCR4-D	KGHQKRKALKTT VILILAFFACWLPYYIGISI	DSFILLEI IKQGEFENTVHK	WISITEA	289
Ref. CXCR4-D	KGHQKRKALKTT VILILAFFACWLPYYIGISI	DSFILLEI IKQGEFENTVHK	WISITEA	322
Ref. CXCR4-C	KGHQKRKALKTT VILILAFFACWLPYYIGISI	DSFILLEI IKQGEFENTVHK	WISITEA	360
Ref. CXCR4-A	KGHQKRKALKTT VILILAFFACWLPYYIGISI	DSFILLEI IKQGEFENTVHK	WISITEA	293
CXCR4-A	KGHQKRKALKTT VILILAFFACWLPYYIGISI	DSFILLEI IKQGEFENTVHK	WISITEA	293
Ref. CXCR4-E	KGHQKRKALKTT VILILAFFACWLPYYIGISI	DSFILLEI IKQGEFENTVHK	WISITEA	274
CXCR4-E	KGHQKRKALKTT VILILAFFACWLPYYIGISI	DSFILLEI IKQGEFENTVHK	WISITEA	274
	*****	*****	*****	*****

```

CLUSTAL O(1.2.4) multiple sequence alignment

          TM7          C-terminal segment
Ref.CXCR4-B  LAFFHCCLNPILY  AFLGAKFKTSAQHALTSVSRGSSLKILSKGKRGGHSSVSTESESSSF  349
CXCR4-B      LAFFHCCLNPILY  AFLGAKFKTSAQHALTSVSRGSSLKILSKGKRGGHSSVSTESESSSF  349
CXCR4-C      LAFFHCCLNPILY  AFLGAKFKTSAQHALTSVSRGSSLKILSKGKRGGHSSVSTESESSSF  349
CXCR4-D      LAFFHCCLNPILY  AFLGAKFKTSAQHALTSVSRGSSLKILSKGKRGGHSSVSTESESSSF  349
Ref.CXCR4-D  LAFFHCCLNPILY  AFLGAKFKTSAQHALTSVSRGSSLKILSKGKRGGHSSVSTESESSSF  382
Ref.CXCR4-C  LAFFHCCLNPILY  AFLGAKFKTSAQHALTSVSRGSSLKILSKGKRGGHSSVSTESESSSF  420
Ref.CXCR4-A  LAFFHCCLNPILY  AFLGAKFKTSAQHALTSVSRGSSLKILSKGKRGGHSSVSTESESSSF  353
CXCR4-A      LAFFHCCLNPILY  AFLGAKFKTSAQHALTSVSRGSSLKILSKGKRGGHSSVSTESESSSF  353
Ref.CXCR4-E  LAFFHCCLNPILY  AFLGAKFKTSAQHALTSVSRGSSLKILSKGKRGGHSSVSTESESSSF  334
CXCR4-E      LAFFHCCLNPILY  AFLGAKFKTSAQHALTSVSRGSSLKILSKGKRGGHSSVSTESESSSF  334
*****

          C-terminal segment
Ref.CXCR4-B  HSS      352
CXCR4-B      HSS      352
CXCR4-C      HSS      352
CXCR4-D      HSS      352
Ref.CXCR4-D  HSS      385
Ref.CXCR4-C  HSS      423
Ref.CXCR4-A  HSS      356
CXCR4-A      HSS      356
Ref.CXCR4-E  HSS      337
CXCR4-E      HSS      337
***

```

Figure 16. The multiple sequence alignment results of translated CXCR4 DNA sequences with reference protein sequences on the NCBI database. Note: conserved sequence (*); conservative mutations (:); and non-conservative mutations ().

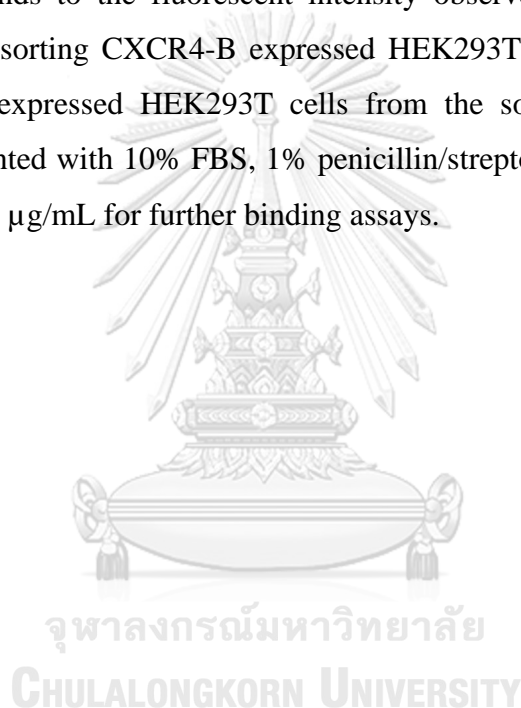
4.1.2. Stable CXCR4 expressing HEK293T cells construction

The CXCR4 isotype B is the most isotype expressed on human cells. The cDNA of a spliced mRNA of CXCR4-B (or leukocyte-derived seven-transmembrane domain receptor (LESTR)) encodes the protein sequence of CXCR4, which is comprised of 352 amino acid (aa) residues, and this receptor is expressed abundantly in human blood monocytes [11, 66]. Although the human CXCR4 gene is expressed in two functional forms: CXCR4-B and CXCR4-A variants, CXCR4-B is considered highly expressed and more abundant than CXCR4-A (also called CXCR4-Lo), which has a 9 aa extension N-segment [67]. Thus, CXCR4-B is considered as a canonical sequence for studies on CXCR4. In this study, the recombinant CXCR4-B-pTriEX™ 1.1 Hygro plasmids were selected to be transfected in HEK293T cells for producing stably CXCR4-overexpressed HEK293T cells.

4.1.3. The isolation of CXCR4-overexpressed cells

The CXCR4 expression on the surface of the CXCR4-B expressed HEK293T cells was evaluated by flow cytometry using the PE-tagged anti-hCD184 antibody, the

CXCR4 expression in the transfected cells showed high fluorescence intensity, compared to the normal HEK293T cells which had low expression of CXCR4 or fluorescent signals (Figure 17-b). The CXCR4 expression on the CXCR4-B expressed HEK293T cell surface is divided into 2 sub-populations: high and low expression populations of 63.6% and 35.1%, respectively (Figure 17-c). The highly expressing cells were further isolated by fluorescence-activated cell sorting (FACS). The highly CXCR4-B expressed HEK293T cells were successfully isolated by FACS showing 99.8% of cells tagged PE-anti hCD184 antibody at high fluorescent intensity (Figure 17-d). It corresponds to the fluorescent intensity observed in the high expression population of pre-sorting CXCR4-B expressed HEK293T as shown in Figure 17-c. The CXCR4-overexpressed HEK293T cells from the sorting were maintained in DMEM supplemented with 10% FBS, 1% penicillin/streptomycin, 1% glutamine and hygromycin B 500 $\mu\text{g}/\text{mL}$ for further binding assays.



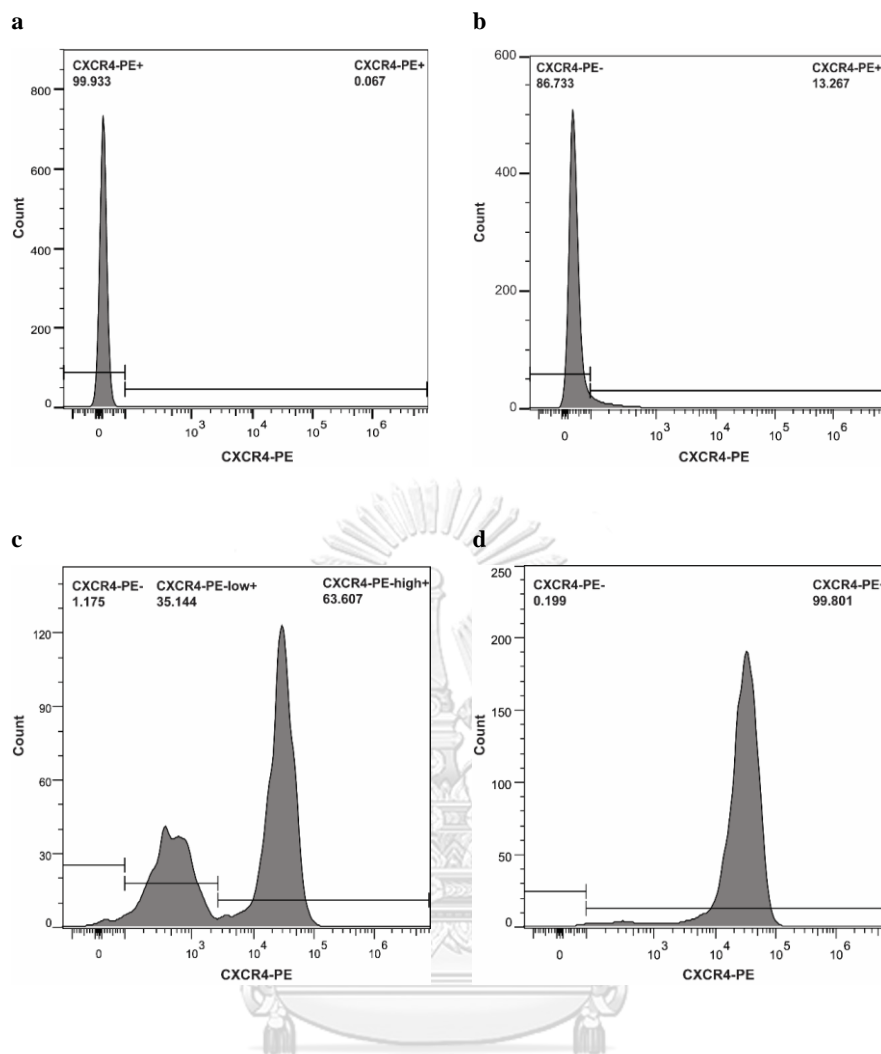


Figure 17. Flow cytometric analysis of (a) unstained CXCR4-B expressed HEK293T cells; (b) normal HEK293T cells stained with PE-conjugated anti-hCD184 antibody; (c) pre-sorting CXCR4-B expressed HEK293T cells stained with PE-conjugated anti-hCD184 antibody and (d) CXCR4-overexpressed HEK293T cells sorted by FACS.

4.2. Verification of CXCR4-overexpressed HEK293T cells

The CXCR4 overexpressing HEK293T cells were assessed for binding assay by (i) determining its binding affinity via the saturation binding assay using the PE-conjugated anti-hCD184 antibody and (ii) determining the binding IC_{50} of the CXCR4 antagonist via a competitive binding assay.

4.2.1. Saturation binding assay using PE-conjugated anti-hCD184 antibody

The saturation binding assay to determine the binding affinity of CXCR4 receptors on the surface of the produced CXCR4-overexpressed HEK293T cells was performed by using PE-conjugated anti-hCD184 antibody. The saturation binding assay of the PE tagged antibody in CXCR4-overexpressing HEK293T cells showed a high binding affinity at EC_{50} of 967.8 pM (Figure 18). The binding results suggest that the CXCR4 expressing HEK293T cells are efficient as a tool for the binding study of CXCR4 ligands.

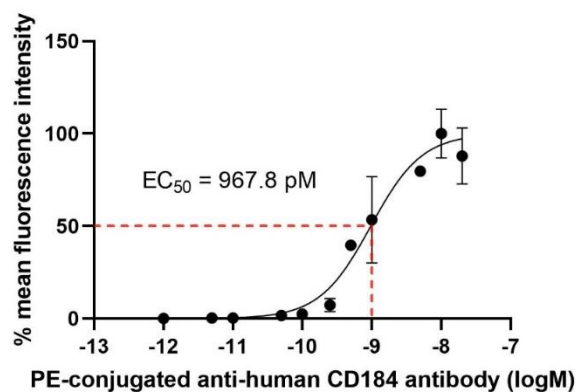


Figure 18. Saturation binding assay of CXCR4 overexpressing HEK293T cells using PE-conjugated anti-hCD184 antibody.

4.2.2. Competitive binding assay of CXCR4 antagonist

A CXCR4 antagonist, AMD3100, was used in the competitive binding assay to determine the IC_{50} . The result showed that AMD3100 could bind to the cell surface CXCR4 as observed by its inhibition against PE-conjugated anti-hCD184 antibody binding at the IC_{50} of 305.5 nM (Figure 19).

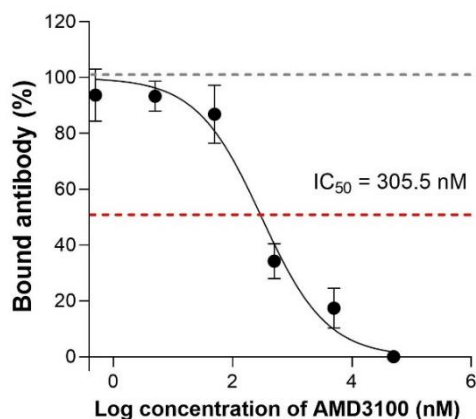


Figure 19. Competitive binding assay of AMD3100 against PE-conjugated anti-hCD184 antibody.

When compared the obtained IC_{50} of AMD3100 with those from other competitive binding assays using different competitive ligands (Table 15), the IC_{50} value from the platform was in agreement with others, within the same order of magnitude, particularly with the same class of competing ligand and the fluorescence probe type. The differences appeared to be only modest, which may be contributed by the variation of experimental conditions or cell types used in the competitive binding assay to determine the binding affinity of CXCR4 ligand

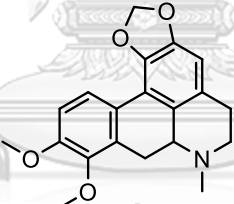
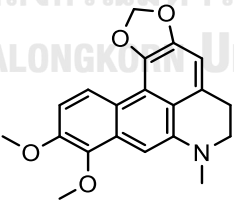
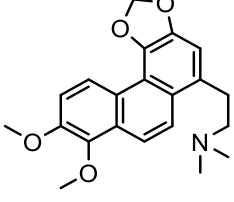
Table 15. IC_{50} values of AMD3100 from different competitive binding assays

Technique	IC_{50}	Probe-Ligand	CXCR4 ⁺ cells	Ref
Radioligand binding				
Radioligand competition	213	[¹²⁵ I]-SDF-1 α	HEK293	[68]
	651	[¹²⁵ I]-SDF-1 α	CCRF-CEM	[69]
Fluorescence ligand binding				
High-affinity peptide competition	314	FITC-CVX15	CHO	[64]
	104	FITC-DV1	CHO	[64]
Antibody-competition	324	FITC-anti hCD184	CHO	[64]
	578	APC-anti hCD184	SupT1	[4]
	305	PE-anti hCD184	HEK293T	this work

4.3. Competitive binding assay of natural compounds to CXCR4

The competitive binding assay CXCR4-overexpressed HEK293T cells were used to determine the binding affinity of potential compounds from the *Stephania pierrei* plant, which were methoxy-8-uvariopsine, crebanine and dehydrocrebanine. The cytotoxic IC_{50} of three compounds in Table 16 showed the potential anticancer activity on invasive breast cancer cell line, MDA-MB-231. Specifically, crebanine has shown the lowest IC_{50} at 0.29 μM to MDA-MB-231, While those from methoxy-8-uvariopsine and dehydrocrebanine were 9.53 μM and 7.27 μM , respectively. As MDA-MB-231 cells have been reported to have high CXCR4 expression [70] so the target mediated cytotoxicity could be CXCR4. Therefore, the competitive binding assay was carried out to determine the binding affinity of these three compounds.

Table 16. The natural compounds of investigation

Compound	Structure	Plant	IC_{50} (MDA-MB 231) (μM)
Crebanine		<i>Stephania pierrei</i>	0.29
Dehydrocrebanine		<i>Stephania pierrei</i>	7.27
Methoxy-8-uvariopsine		<i>Stephania pierrei</i>	9.53

In the binding assays, the tested concentrations were initially in the range of 0.5 to 50 μM in PBS, and the results and AMD3100, a CXCR4 antagonist and clonidine were used as reference compounds.

As presented in Figure 20, the decrease in the intensities of PE-tagged CXCR4 antibody bound CXCR4 was not observed, so these two compounds may not bind to CXCR4. However, it was found that partial precipitation occurred when diluting the stock solution (0.1 mg/mL in DMSO) with PBS leading to a minute concentration of the test compound in the assay wells. Therefore, the diluted solvents were changed to 100% DMSO and/or 0.5% Tween 20 + 0.5% DMSO in the later trials to improve the solubility. In addition, the concentrations of the 4 compounds tested were increased to 100, 200 and 400 μM , except for dehydrocrebanine, which was tested at 500 and 1000 μM . The competitive binding assays with modified vehicles to avoid precipitation showed a much lower fluorescence intensity of bound PE-tagged antibodies than those from PBS vehicles. The fluorescent quenching was possibly the cause of low fluorescent intensities as fluorescent quenching of DMSO (greater than 1%), and Tween 20 have been reported, particularly Tween has been used as fluorescent quenching agent [71]. In addition, the high concentration of the test compound may also interfere with the binding.

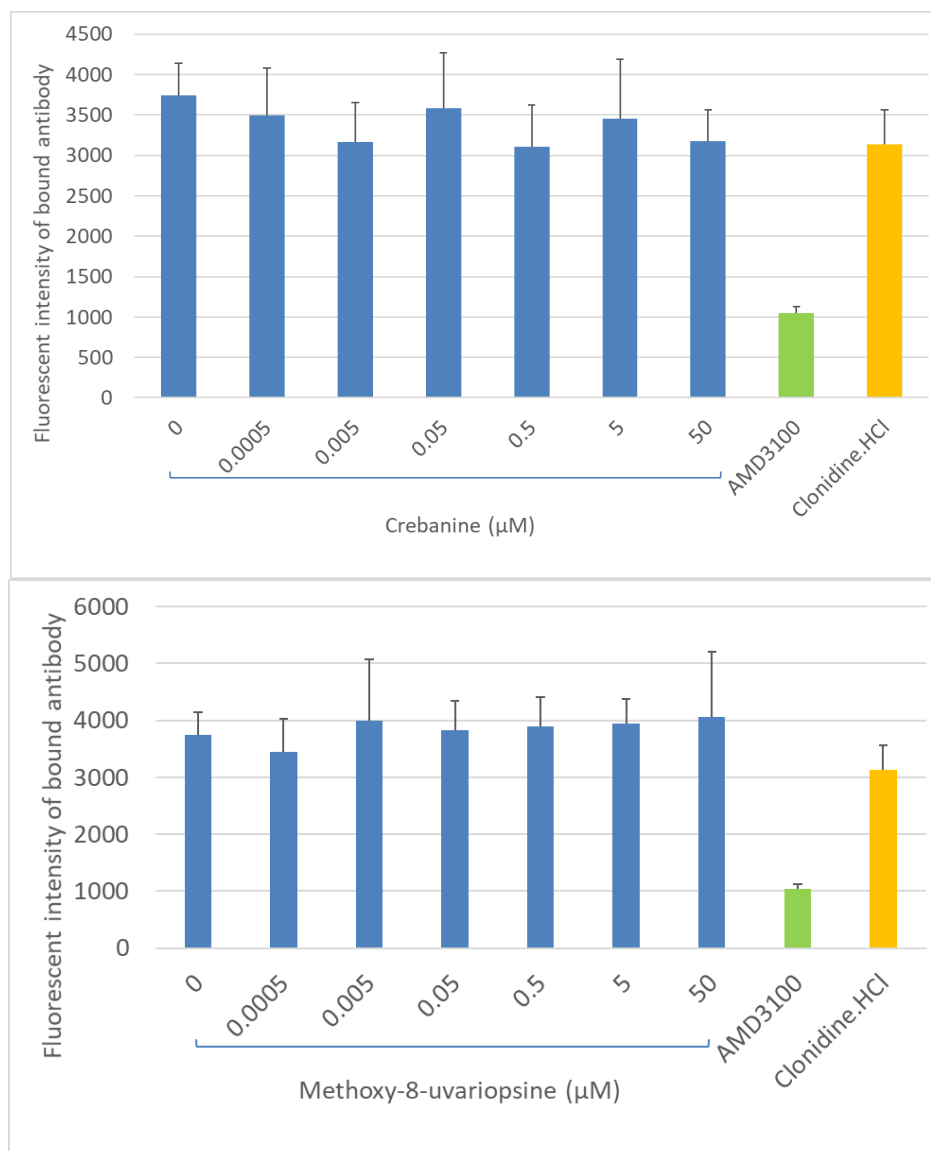


Figure 20. Competitive binding assay of crebanine and methoxy-8-uvariopsine diluted in PBS using PE-conjugated anti-hCD184 antibody and CXCR4-overexpressed HEK293T cells. The concentration of reference CXCR4 antagonist (AMD3100) and clonidine was 305.5 nM

CHAPTER 5. CONCLUSION

In this study, the construction of recombinant CXCR4 plasmids and the production of stably CXCR4 overexpressing HEK293T cells for binding assay have been achieved with over 99% CXCR4 expression and high CXCR4 binding affinity at a picomolar level. The CXCR4 overexpressing HEK293T cells were used in the fluorescence tagged antibody competition binding assay to determine the binding affinity of the CXCR4 antagonist, AMD3100, and the obtained binding IC_{50} value of AMD3100 was in agreement with the conventional radioligand binding assay. This result verified the use of produced CXCR4 overexpressing HEK293T cells in the binding assays. Thus, the developed CXCR4 overexpressing HEK293T cell line has great potential as a platform for competitive binding assays of potential anti-cancer agents targeting CXCR4. This platform was employed to determine the mechanism of four potential compounds showing promising cytotoxicity against CXCR4 expressing breast cancer cell line (MDA-MB-231). However, several attempts have been tried without success due to poor solubility. In addition, the high fluorescence quenching and the interferences from the solvent and high concentration of test compound are the crucial factors limiting the application of the fluorescence tagged antibody competition binding assay in binding affinity determination.

The prospective study will be the development of a fluorescence tagged CXCR4-antagonist to reduce the assay cost and the exploration for the anti-quenching vehicle for screening the poor soluble compounds from the plant.

APPENDICES

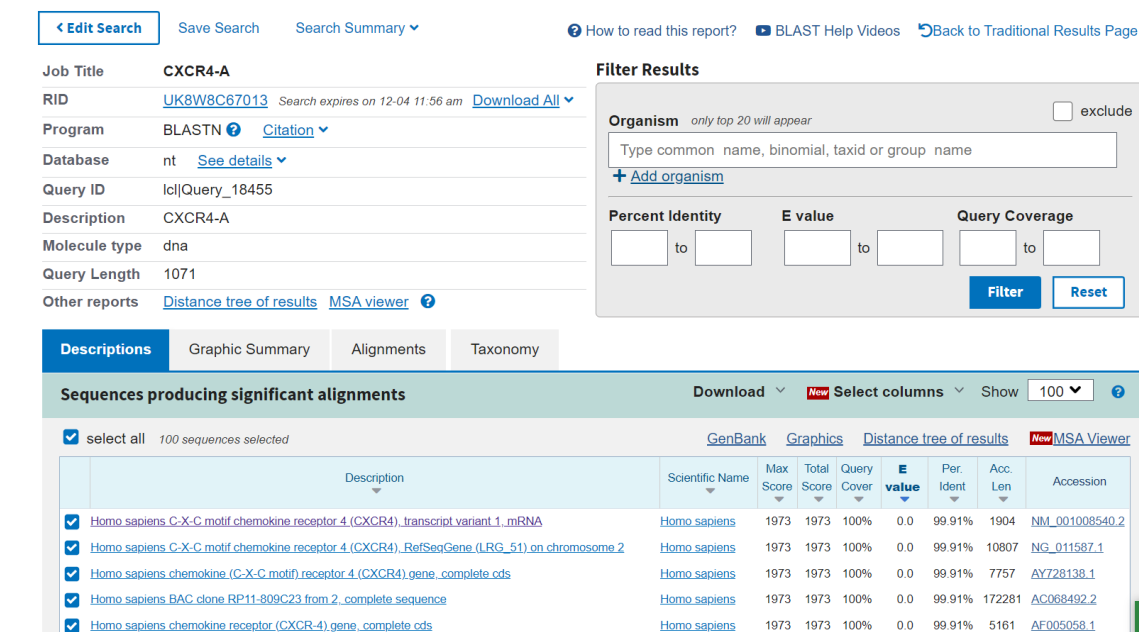


Figure A1. BLAST results of CXCR4-A sequence

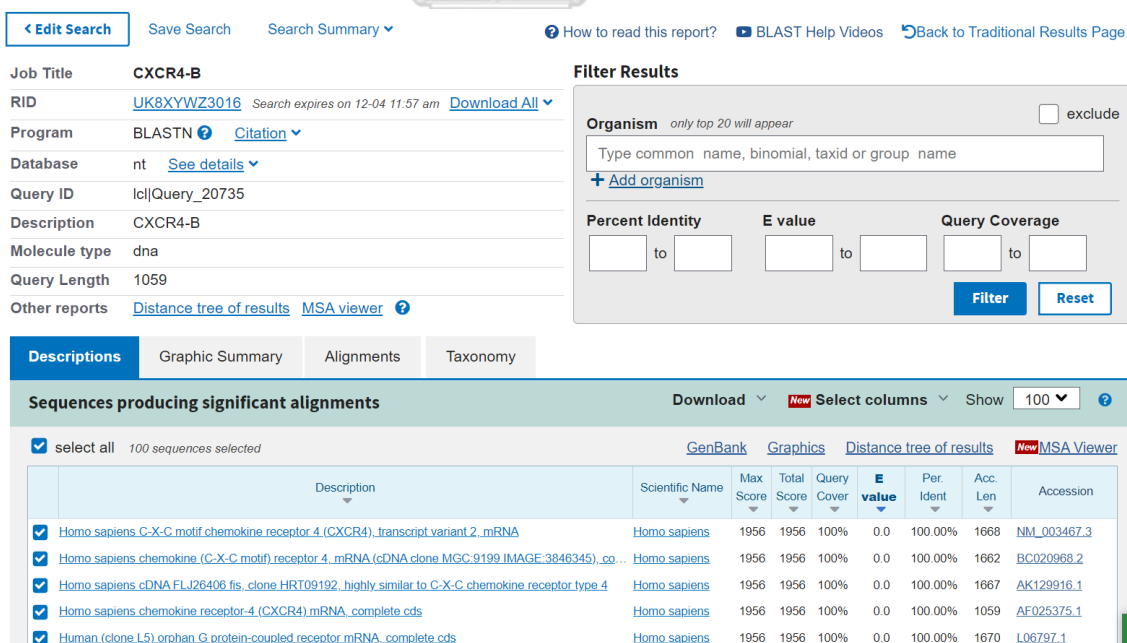


Figure A2. BLAST results of CXCR4-B sequence

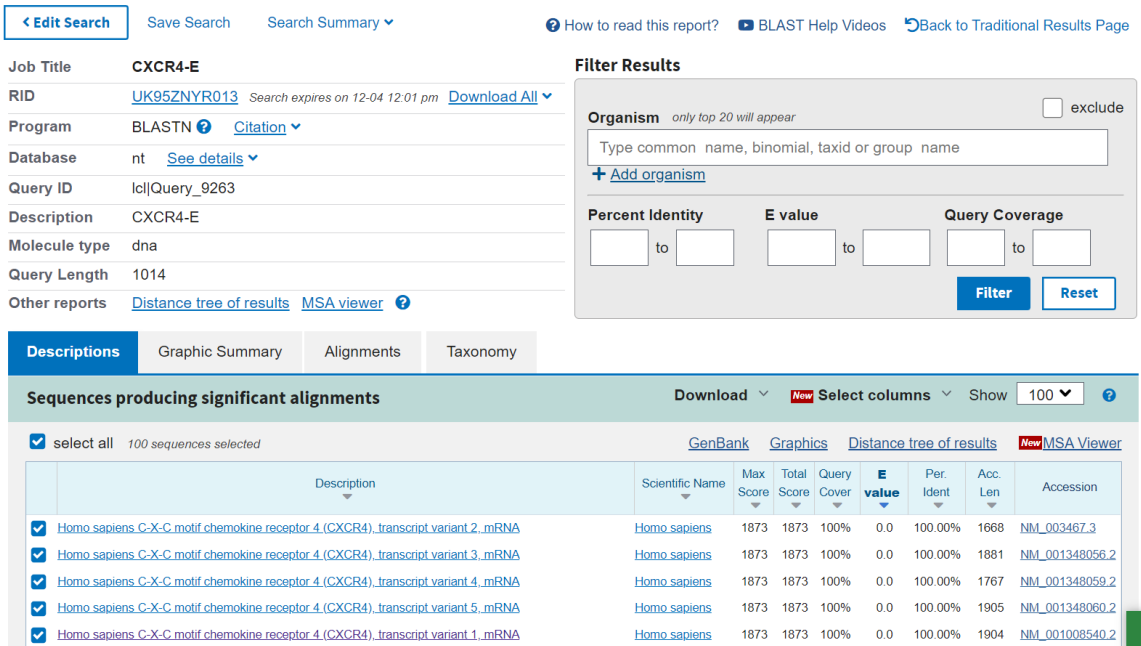


Figure A3. BLAST results of CXCR4-E sequence

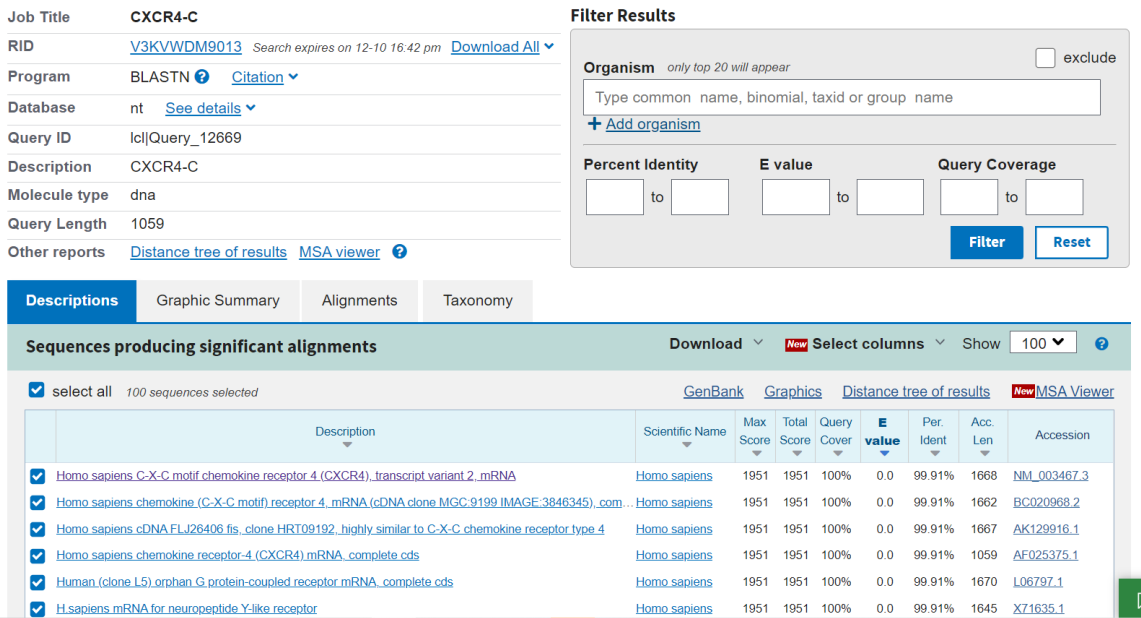


Figure A4. BLAST results of CXCR4-C sequence

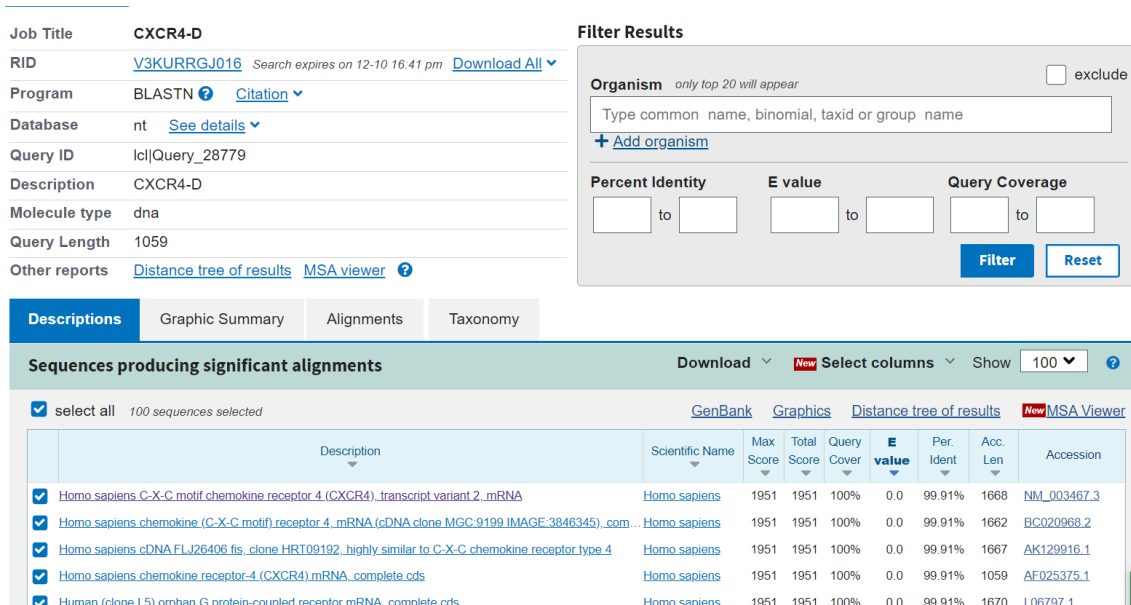


Figure A5. BLAST results of CXCR4-D sequence

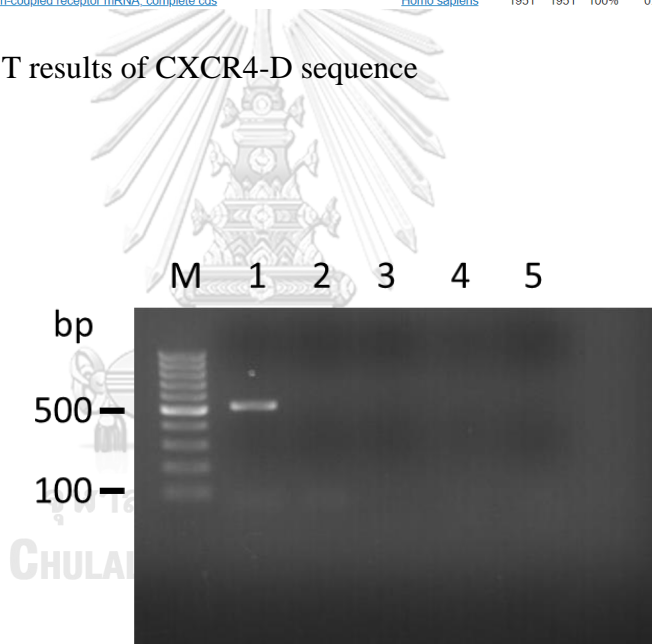


Figure A6. Mycoplasma contamination test of CXCR4-B-overexpressed HEK293T cells. Lane M: GeneRuler™ 100 bp DNA ladder; Lane 1: Positive control (DNA of Mycoplasma bacteria); Lane 2: Negative control (Nuclease-free water); Lane 3-5: Negative results of CXCR4-B overexpressed HEK293T clone 1-3, respectively. Numbers at the left are DNA sizes in bp.

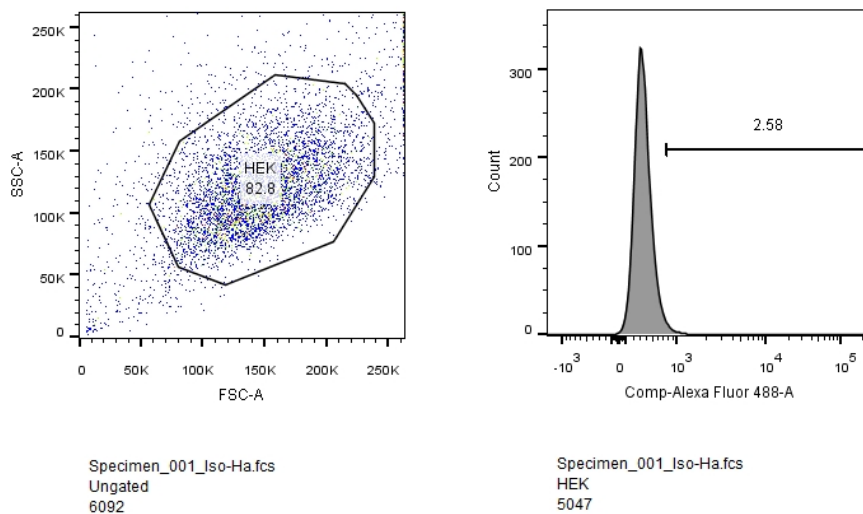
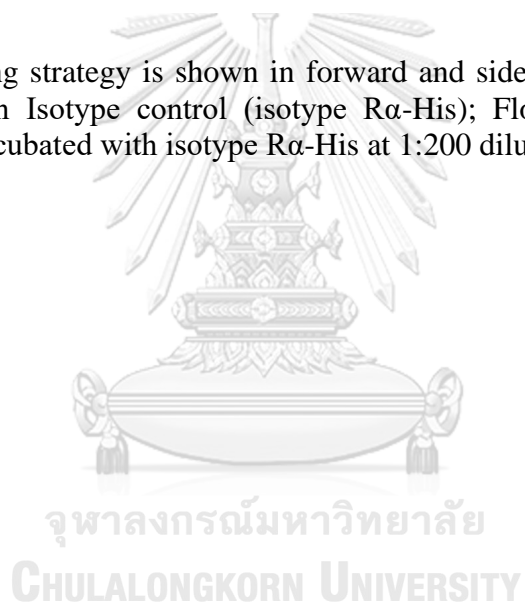


Figure A7. Gating strategy is shown in forward and side scatter with 82.8% intact HEK293T cells in Isotype control (isotype $R\alpha$ -His); Flow cytometry analysis of HEK293T cells incubated with isotype $R\alpha$ -His at 1:200 dilution.



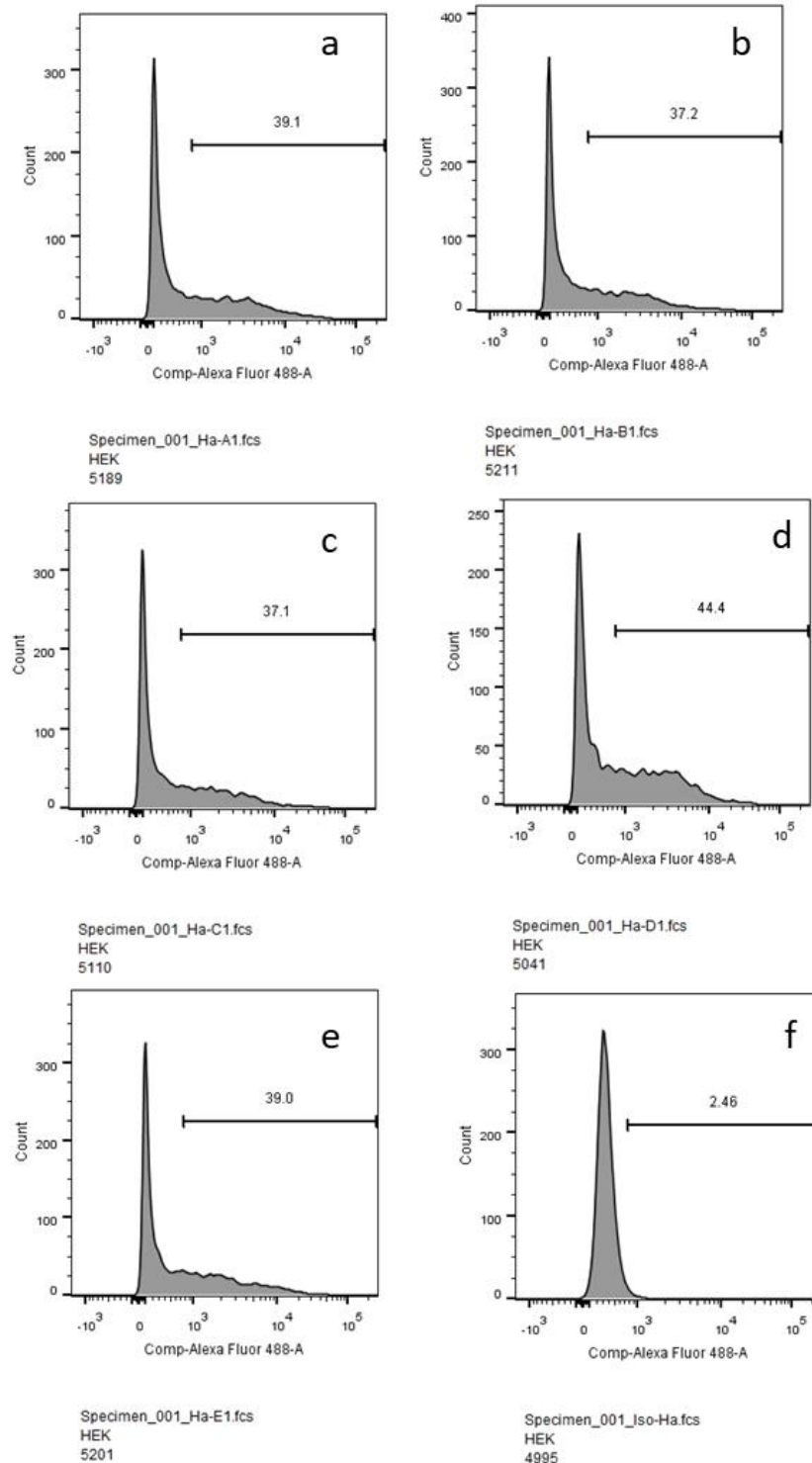


Figure A8. Flow cytometry analysis of HEK293T cells transiently transfected with CXCR4 isotype A9, B6, C2, D1 and E12 respectively incubated with anti-CXCR4 antibody [UMB2] at 1:200 dilution (a, b, c, d and e); Flow cytometry analysis of HEK293T cells incubated with isotype R α -His at 1:200 dilution (f).

1st trial

CXCR4+HEK293T	MFI	MFI-BG		HEK293T	MFI	MFI-BG	
Background (PBS)	93.33	0.00		Background (PBS)	87.67	0.00	
AMD3100 (305.5 nM)	1590.00	1496.67		AMD3100 (305.5 nM)	537.33	449.67	
Clonidine.HCl (305.5 nM)	3660.00	3566.67		Clonidine.HCl (305.5 nM)	518.00	430.33	
Crebanine (DMSO+PBS)				Crebanine (DMSO+PBS)			
0 nM	4067.00	3973.67		0 nM	317.67	230.00	
0.5 nM	3843.33	3750.00		0.5 nM	347.00	259.33	
5 nM	3685.00	3591.67		5 nM	518.33	430.67	
50 nM	4025.67	3932.33		50 nM	436.33	348.67	
500 nM	3612.00	3518.67		500 nM	495.33	407.67	
5 μ M	4008.33	3915.00		5 μ M	553.67	466.00	
50 μ M	3639.00	3545.67		50 μ M	460.67	373.00	

2nd trial

CXCR4+HEK293T	MFI	MFI-BG		HEK293T	MFI	MFI-BG	
Background (PBS)	71.33	0.00		Background (PBS)	61.33	0.00	
AMD3100 (305.5 nM)	4707.00	4635.67		AMD3100 (305.5 nM)	338.33	277.00	
Clonidine.HCl (305.5 nM)	4888.00	4816.67		Clonidine.HCl (305.5 nM)	420.67	359.33	
BG (DMSO)	63.00	0.00		BG (DMSO)	51.00	0.00	
Crebanine (DMSO)				Crebanine (DMSO)			
0 μ M	169.67	106.67	Fluorescent quenching	0 μ M	168.67	117.67	
1 μ M	159.00	96.00	Fluorescent quenching	1 μ M	187.67	136.67	
10 μ M	233.67	170.67	Fluorescent quenching	10 μ M	192.00	141.00	
50 μ M	243.00	180.00	Fluorescent quenching	50 μ M	235.67	184.67	
100 μ M	226.00	163.00	Fluorescent quenching	100 μ M	217.33	166.33	
200 μ M	325.33	262.33	Fluorescent quenching	200 μ M	260.67	209.67	
400 μ M	349.33	286.33	Fluorescent quenching	400 μ M	189.67	138.67	

3rd trial

CXCR4+HEK293T	MFI	MFI-BG		HEK293T	MFI	MFI-BG	
Background (PBS)	68.67	0.00		Background (PBS)	70.33	0.00	
AMD3100 (305.5 nM)	2664.33	2595.67		AMD3100 (305.5 nM)	199.67	129.33	
Clonidine.HCl (305.5 nM)	5698.33	5629.67		Clonidine.HCl (305.5 nM)	162.67	92.33	
PE-antiCD184 (5 nM)	5542.33	5473.67		PE-antiCD184 (5 nM)	260.33	190.00	
BG (DMSO+Tween)	76.33	0.00		BG (DMSO+Tween)	70.33	0.00	
Crebanine (DMSO+Tween)				Crebanine (DMSO+Tween)			
0 μ M	289.00	212.67	Fluorescent quenching	0 μ M	239.33	169.00	
1 μ M	296.67	220.33	Fluorescent quenching	1 μ M	176.67	106.33	
10 μ M	236.00	159.67	Fluorescent quenching	10 μ M	224.00	153.67	
50 μ M	422.00	345.67	Fluorescent quenching	50 μ M	216.00	145.67	
100 μ M	459.33	383.00	Fluorescent quenching	100 μ M	218.33	148.00	
200 μ M	834.67	758.33	Fluorescent quenching	200 μ M	228.67	158.33	

Figure A9. Results of competitive binding assays of crebanine and PE-conjugated anti-hCD184 antibody in CXCR4-overexpressed HEK293T cells.

1st trial

CXCR4+HEK293T	MFI	MFI-BG		HEK293T	MFI	MFI-BG	
Background (PBS)	93.33	0.00		Background (PBS)	87.67	0.00	
AMD3100 (305.5 nM)	1590.00	1496.67		AMD3100 (305.5 nM)	537.33	449.67	
Clonidine.HCl (305.5 nM)	3660.00	3566.67		Clonidine.HCl (305.5 nM)	518.00	430.33	
Methoxy-8-uvariopsine (DMSO+PBS)				Methoxy-8-uvariopsine (DMSO+PBS)			
0 nM	4067.00	3973.67		0 nM	317.67	230.00	
0.5 nM	4218.67	4125.33		0.5 nM	758.67	671.00	
5 nM	4660.33	4567.00		5 nM	664.67	577.00	
50 nM	4328.33	4235.00		50 nM	503.00	415.33	
500 nM	4776.00	4682.67		500 nM	868.33	780.67	
5 μ M	4770.33	4677.00		5 μ M	813.67	726.00	
50 μ M	4589.00	4495.67		50 μ M	525.33	437.67	

2nd trial

CXCR4+HEK293T	MFI	MFI-BG		HEK293T	MFI	MFI-BG	
Background (PBS)	71.33	0.00		Background (PBS)	61.33	0.00	
AMD3100 (305.5 nM)	4707.00	4635.67		AMD3100 (305.5 nM)	338.33	277.00	
Clonidine.HCl (305.5 nM)	4888.00	4816.67		Clonidine.HCl (305.5 nM)	420.67	359.33	
BG (DMSO)	63.00	0.00		BG (DMSO)	51.00	0.00	
Methoxy-8-uvariopsine (DMSO)				Methoxy-8-uvariopsine (DMSO)			
0 μ M	169.67	106.67	Fluorescent quenching	0 μ M	168.67	117.67	
1 μ M	165.00	102.00	Fluorescent quenching	1 μ M	253.33	202.33	
10 μ M	152.33	89.33	Fluorescent quenching	10 μ M	214.67	163.67	
50 μ M	147.00	84.00	Fluorescent quenching	50 μ M	272.00	221.00	
100 μ M	170.67	107.67	Fluorescent quenching	100 μ M	170.00	119.00	
200 μ M	188.67	125.67	Fluorescent quenching	200 μ M	354.00	303.00	
400 μ M	230.00	167.00	Fluorescent quenching	400 μ M	229.33	178.33	

3rd trial

CXCR4+HEK293T	MFI	MFI-BG		HEK293T	MFI	MFI-BG	
Background (PBS)	68.67	0.00		Background (PBS)	70.33	0.00	
AMD3100 (305.5 nM)	2664.33	2595.67		AMD3100 (305.5 nM)	199.67	129.33	
Clonidine.HCl (305.5 nM)	5698.33	5629.67		Clonidine.HCl (305.5 nM)	162.67	92.33	
PE-antiCD184 (5 nM)	5542.33	5473.67		PE-antiCD184 (5 nM)	260.33	190.00	
BG (DMSO+Tween)	76.33	0.00		BG (DMSO+Tween)	70.33	0.00	
Methoxy-8-uvariopsine (DMSO+Tween)				Methoxy-8-uvariopsine (DMSO+Tween)			
0 μ M	289.00	212.67	Fluorescent quenching	0 μ M	239.33	169.00	
1 μ M	353.67	277.33	Fluorescent quenching	1 μ M	251.00	180.67	
10 μ M	288.00	211.67	Fluorescent quenching	10 μ M	227.67	157.33	
50 μ M	428.00	351.67	Fluorescent quenching	50 μ M	222.67	152.33	
100 μ M	420.00	343.67	Fluorescent quenching	100 μ M	201.67	131.33	
200 μ M	434.00	357.67	Fluorescent quenching	200 μ M	246.33	176.00	

Figure A10. Results of competitive binding assays of methoxy-8-uvariopsine and PE-conjugated anti-hCD184 antibody in CXCR4-overexpressed HEK293T cells.

2nd trial

CXCR4+HEK293T	MFI	MFI-BG		HEK293T	MFI	MFI-BG	
Background (PBS)	71.33	0.00		Background (PBS)	61.33	0.00	
AMD3100 (305.5 nM)	4707.00	4635.67		AMD3100 (305.5 nM)	338.33	277.00	
Clonidine.HCl (305.5 nM)	4888.00	4816.67		Clonidine.HCl (305.5 nM)	420.67	359.33	
BG (DMSO)	63.00	0.00		BG (DMSO)	51.00	0.00	
Dydrocrebanine (DMSO)				Dydrocrebanine (DMSO)			
0 μ M	169.67	106.67	Fluorescent quenching	0 μ M	168.67	117.67	
500 μ M	214.00	151.00	Fluorescent quenching	500 μ M	204.67	153.67	
1000 μ M	264.00	201.00	Fluorescent quenching	1000 μ M	232.33	181.33	

3rd trial

CXCR4+HEK293T	MFI	MFI-BG		HEK293T	MFI	MFI-BG	
Background (PBS)	68.67	0.00		Background (PBS)	70.33	0.00	
AMD3100 (305.5 nM)	2664.33	2595.67		AMD3100 (305.5 nM)	199.67	129.33	
Clonidine.HCl (305.5 nM)	5698.33	5629.67		Clonidine.HCl (305.5 nM)	162.67	92.33	
PE-antiCD184 (5 nM)	5542.33	5473.67		PE-antiCD184 (5 nM)	260.33	190.00	
BG (DMSO+Tween)	76.33	0.00		BG (DMSO+Tween)	70.33	0.00	
Dydrocrebanine (DMSO+Tween)				Dydrocrebanine (DMSO+Tween)			
0 μ M	289.00	212.67	Fluorescent quenching	0 μ M	239.33	169.00	
1 μ M	320.33	244.00	Fluorescent quenching	1 μ M	240.00	169.67	
10 μ M	350.00	273.67	Fluorescent quenching	10 μ M	200.33	130.00	
50 μ M	384.33	308.00	Fluorescent quenching	50 μ M	217.67	147.33	
100 μ M	359.67	283.33	Fluorescent quenching	100 μ M	252.33	182.00	
200 μ M	406.00	329.67	Fluorescent quenching	200 μ M	164.67	94.33	

Figure A11. Results of competitive binding assays of dehydrocrebanine and PE-conjugated anti-hCD184 antibody in CXCR4-overexpressed HEK293T cells.

REFERENCES



จุฬาลงกรณ์มหาวิทยาลัย
CHULALONGKORN UNIVERSITY

1. Bleul CA, Wu L, Hoxie JA, Springer TA, Mackay CR. The HIV coreceptors CXCR4 and CCR5 are differentially expressed and regulated on human T lymphocytes. *Proc Natl Acad Sci USA*. 1997;94:1925-30.
2. Lee B, Sharron M, Montaner L, Weissman D, Doms RW. Quantification of CD4, CCR5, and CXCR4 levels on lymphocyte subsets, dendritic cells, and differentially conditioned monocyte-derived macrophages. *Proc Natl Acad Sci USA*. 1999;96:5215-20.
3. Zhou Y, Cao H-B, Li W-J, Zhao L. The CXCL12 (SDF-1)/CXCR4 chemokine axis: Oncogenic properties, molecular targeting, and synthetic and natural product CXCR4 inhibitors for cancer therapy. *Chin J Nat Med*. 2018;16(11):801-10.
4. Harms M, Gilg A, Standker L, Beer AJ, Mayer B, Rasche V, et al. Microtiter plate-based antibody-competition assay to determine binding affinities and plasma/blood stability of CXCR4 ligands. *Sci Rep*. 2020;10(1):16036.
5. Teixido J, Martinez-Moreno M, Diaz-Martinez M, Sevilla-Movilla S. The good and bad faces of the CXCR4 chemokine receptor. *Int J Biochem Cell Biol*. 2018;95:121-31.
6. Zhou W, Guo S, Liu M, Burow ME, Wang G. Targeting CXCL12/CXCR4 axis in tumor immunotherapy. *Curr Med Chem*. 2019;26(17):3026-41.
7. Atwood BK, Lopez J, Wager-Miller J, Mackie K, Straiker A. Expression of G protein-coupled receptors and related proteins in HEK293, AtT20, BV2, and N18 cell lines as revealed by microarray analysis. *BMC Genomics*. 2011;12:14.
8. Parsi B, Esmaili A, Hashemi M, Behjati M. Transient expression of recombinant ACKR4 (CCRL1) gene, an atypical chemokine receptor in human embryonic kidney (HEK 293) cells. *Mol Biol Rep*. 2016;43(7):583-9.
9. Thomas P, Smart TG. HEK293 cell line: a vehicle for the expression of recombinant proteins. *J Pharmacol Toxicol Methods*. 2005;51(3):187-200.
10. Congreve M, Dias JM, Marshall FH. Structure-based drug design for G protein-coupled receptors. *Prog Med Chem*. 2014;53:1-63.
11. Loetscher M, Geiser T, O'Reilly T, Zwahlen R, Baggiolini M, Moser B. Cloning of a human seven-transmembrane domain receptor, LESTR, that is highly expressed in leukocytes. *J Biol Chem*. 1994;269:232-7.

12. Oberlin E, Amara A, Bachelier Fo, Bessia C, Virelizier J-L, Arenzana-Seisdedos F, et al. The CXC chemokine SDF-1 is the ligand for LESTR/fusin and prevents infection by T-cell-line-adapted HIV-1. *Nature*. 1996;382(6594):833-5.
13. Scholten DJ, Canals M, Maussang D, Roumen L, Simit MJ, Wijtmans M, et al. Pharmacological modulation of chemokine receptor function. *Br J Pharmacol*. 2012;165(6):1617-43.
14. Soave M, Heukers R, Kellam B, Woolard J, Smit MJ, Bridson SJ, et al. Monitoring allosteric interactions with CXCR4 using nanoBiT conjugated nanobodies. *Cell Chem Biol*. 2020;27(10):1250-61 e5.
15. Teicher BA, Fricker SP. CXCL12 (SDF-1)/CXCR4 pathway in cancer. *Clin Cancer Res*. 2010;16(11):2927-31.
16. Wescott MP, Kufareva I, Paes C, Goodman JR, Thaker Y, Puffer BA, et al. Signal transmission through the CXC chemokine receptor 4 (CXCR4) transmembrane helices. *Proc Natl Acad Sci USA*. 2016;113(35):9928-33.
17. Yang Y, Zhang Q, Gao M, Yang X, Huang Z, An J. A novel CXCR4-selective high-affinity fluorescent probe and its application in competitive binding assays. *Biochemistry*. 2014;53(30):4881-3.
18. Shin HN, Moon HH, Ku JL. Stromal cell-derived factor-1alpha and macrophage migration-inhibitory factor induce metastatic behavior in CXCR4-expressing colon cancer cells. *Int J Mol Med*. 2012;30(6):1537-43.
19. Saini V, Staren DM, Ziarek JJ, Nashaat ZN, Campbell EM, Volkman BF, et al. The CXC chemokine receptor 4 ligands ubiquitin and stromal cell-derived factor-1alpha function through distinct receptor interactions. *J Biol Chem*. 2011;286(38):33466-77.
20. Xu C, Zhao H, Chen H, Yao Q. CXCR4 in breast cancer: oncogenic role and therapeutic targeting. *Drug Des Devel Ther*. 2015;9:4953-64.
21. Park B, Sung B, Yadav VR, Cho SG, Liu M, Aggarwal BB. Acetyl-11-keto-beta-boswellic acid suppresses invasion of pancreatic cancer cells through the downregulation of CXCR4 chemokine receptor expression. *Int J Cancer*. 2011;129(1):23-33.
22. Siegel RL, Miller KD, Fuchs HE, Jemal A. Cancer Statistics, 2021. *CA Cancer J Clin*. 2021;71(1):7-33.

23. Nindrea RD, Aryandono T, Lazuardi L. Breast cancer risk from modifiable and non-modifiable risk factors among women in Southeast Asia: A meta-analysis. *Asian Pac J Cancer Prev.* 2017;18(12):3201-6.
24. Polyak K. Heterogeneity in breast cancer. *J Clin Invest.* 2011;121(10):3786-8.
25. Müller A, Homey B, Soto H, Ge N, Catron D, Buchanan ME, et al. Involvement of chemokine receptors in breast cancer metastasis. *Nature.* 2001;410(6824):50-6.
26. Domanska UM, Kruizinga RC, Nagengast WB, Timmer-Bosscha H, Huls G, de Vries EG, et al. A review on CXCR4/CXCL12 axis in oncology: no place to hide. *Eur J Cancer.* 2013;49(1):219-30.
27. Salvucci O, Bouchard A, Baccarelli A, Deschenes J, Sauter G, Simon R, et al. The role of CXCR4 receptor expression in breast cancer: a large tissue microarray study. *Breast Cancer Res Treat.* 2006;97(3):275-83.
28. Holm NT, Byrnes K, Li BDL, Turnage RH, Abreo F, Mathis JM, et al. Elevated levels of chemokine receptor CXCR4 in HER-2 negative breast cancer specimens predict recurrence. *J Surg Res.* 2007;141(1):53-9.
29. Chu QD, Panu L, Holm NT, Li BD, Johnson LW, Zhang S. High chemokine receptor CXCR4 level in triple negative breast cancer specimens predicts poor clinical outcome. *J Surg Res.* 2010;159(2):689-95.
30. Tahirovic YA, Pelly S, Jecs E, Miller EJ, Sharma SK, Liotta DC, et al. Small molecule and peptide-based CXCR4 modulators as therapeutic agents. A patent review for the period from 2010 to 2018. *Expert Opin Ther Pat.* 2020;30(2):87-101.
31. Song JS, Chang CC, Wu CH, Dinh TK, Jan JJ, Huang KW, et al. A highly selective and potent CXCR4 antagonist for hepatocellular carcinoma treatment. *Proc Natl Acad Sci USA.* 2021;118(13).
32. Stone ND, Dunaway SB, Flexner C, Tierney C, Calandra GB, Becker S, et al. Multiple-dose escalation study of the safety, pharmacokinetics, and biologic activity of oral AMD070, a selective CXCR4 receptor inhibitor, in human subjects. *Antimicrob Agents Chemother.* 2007;51(7):2351-8.
33. Masuda M, Nakashima H, Ueda T, Naba H, Ikoma R, Otaka A, et al. A novel anti-HIV synthetic peptide, T-22 ([Tyr^{5,12},Lys⁷]-polyphemusin II). *Biochem Biophys Res Commun.* 1992;189(2):845-50.

34. Hennrich U, Seyler L, Schafer M, Bauder-Wust U, Eisenhut M, Semmler W, et al. Synthesis and in vitro evaluation of ^{68}Ga -DOTA-4-FBn-TN14003, a novel tracer for the imaging of CXCR4 expression. *Bioorg Med Chem*. 2012;20(4):1502-10.
35. Tamamura H, Xu Y, Hattori T, Zhang X, Arakaki R, Kanbara K, et al. A low-molecular-weight inhibitor against the chemokine receptor CXCR4: a strong anti-HIV peptide T140. *Biochem Biophys Res Commun*. 1998;253(3):877-82.
36. Debnath B, Xu S, Grande F, Garofalo A, Neamati N. Small molecule inhibitors of CXCR4. *Theranostics*. 2013;3(1):47-75.
37. Grande F, Giancotti G, Ioele G, Occhiuzzi MA, Garofalo A. An update on small molecules targeting CXCR4 as starting points for the development of anti-cancer therapeutics. *Eur J Med Chem*. 2017;139:519-30.
38. Murakami T, Nakajima T, Koyanagi Y, Tachibana K, Fujii N, Tamamura H, et al. A small molecule CXCR4 inhibitor that blocks T cell line-tropic HIV-1 infection. *J Exp Med*. 1997;186(8):1389-93.
39. Huang EH, Singh B, Cristofanilli M, Gelovani J, Wei C, Vincent L, et al. A CXCR4 antagonist CTCE-9908 inhibits primary tumor growth and metastasis of breast cancer. *J Surg Res*. 2009;155(2):231-6.
40. Fujii N, Oishi S, Hiramatsu K, Araki T, Ueda S, Tamamura H, et al. Molecular-size reduction of a potent CXCR4-chemokine antagonist using orthogonal combination of conformation- and sequence-based libraries. *Angewandte Chemie (International ed in English)*. 2003;42(28):3251-3.
41. Wang Y, Liang WC, Pan WL, Law WK, Hu JS, Ip DT, et al. Silibinin, a novel chemokine receptor type 4 antagonist, inhibits chemokine ligand 12-induced migration in breast cancer cells. *Phytomedicine*. 2014;21(11):1310-7.
42. Chen XP, Qian LL, Jiang H, Chen JH. Ginsenoside Rg3 inhibits CXCR4 expression and related migrations in a breast cancer cell line. *Int J Clin Oncol*. 2011;16(5):519-23.
43. Kim B, Park B. Baohuoside I suppresses invasion of cervical and breast cancer cells through the downregulation of CXCR4 chemokine receptor expression. *Biochemistry*. 2014;53(48):7562-9.

44. Heng HL, Chee CF, Chin SP, Ouyang Y, Wang H, Buckle MJC, et al. Synthesis and evaluation of nuciferine and roemerine enantiomers as 5-HT₂ and alpha₁ receptor antagonists. *MedChemComm*. 2018;9(3):576-82.
45. Rayanil KO, Prempre C, Nimgirawath S. The first total syntheses of (+/-)-norphoebine, dehydrophoebine, oxophoebine, dehydrocrebanine, oxocrebanine and uthongine and their cytotoxicity against three human cancer cell lines. *J Asian Nat Prod Res*. 2016;18(11):1042-56.
46. Stevigny C, Bailly C, Quetin-Leclercq J. Cytotoxic and antitumor potentialities of aporphinoid alkaloids. *Curr Med Chem Anticancer Agents*. 2005;5(2):173-82.
47. Rodriguez-Arce E, Cancino P, Arias-Calderon M, Silva-Matus P, Saldias M. Oxoisoporphines and aporphines: versatile molecules with anticancer effects. *Molecules*. 2019;25(1).
48. Gerhardt D, Bertola G, Dietrich F, Figueiro F, Zanotto-Filho A, Moreira Fonseca JC, et al. Boldine induces cell cycle arrest and apoptosis in T24 human bladder cancer cell line via regulation of ERK, AKT, and GSK-3beta. *Urol Oncol*. 2014;32(1):36 e1-9.
49. Subramaniam N, Kannan P, K A, Thiruvengadam D. Hepatoprotective effect of boldine against diethylnitrosamine-induced hepatocarcinogenesis in wistar rats. *J Biochem Mol Toxicol*. 2019;33(12):e22404.
50. Paydar M, Kamalidehghan B, Wong YL, Wong WF, Looi CY, Mustafa MR. Evaluation of cytotoxic and chemotherapeutic properties of boldine in breast cancer using in vitro and in vivo models. *Drug Des Devel Ther*. 2014;8:719-33.
51. Leboeuf M, Cave A. Alcaloides des ecorces de l'uvariopsis guineensis. *Phytochemistry*. 1972;11:2833-40.
52. Chaichompoo W, Rojsitthisak P, Pabuprapap W, Siriwattanasathien Y, Yotmanee P, Haritakun W, et al. Stephapierrines A–H, new tetrahydroprotoberberine and aporphine alkaloids from the tubers of *Stephania pierrei* Diels and their anti-cholinesterase activities. *RSC Advances*. 2021;11(34):21153-69.
53. Wongsirisin P, Yodkeeree S, Pompimon W, Limtrakul P. Induction of G1 arrest and apoptosis in human cancer cells by crebanine, an alkaloid from *Stephania venosa*. *Chem Pharm Bull*. 2012;60(10):1283-9.

54. Yodkeeree S, Pompimon W, Limtrakul P. Crebanine, an aporphine alkaloid, sensitizes TNF-alpha-induced apoptosis and suppressed invasion of human lung adenocarcinoma cells A549 by blocking NF-kappaB-regulated gene products. *Tumour Biol.* 2014;35(9):8615-24.
55. Rojsanga P, Boonyarat C, Utsintong M, Nemezc A, Yamauchi JG, Talley TT, et al. The effect of crebanine on memory and cognition impairment via the alpha-7 nicotinic acetylcholine receptor. *Life Sci.* 2012;91(3-4):107-14.
56. Loi VD, Nam PG, Tung BT, Vung NT. Cytotoxic effects in vitro and in vivo of *Stephania glabra* (Roxb.) Miers growing in Vietnam. *World J Medical Sci.* 2017;14(4):121-8.
57. Makarasen A, Sirithana W, Mogkhuntod S, Khunnawutmanotham N, Chimnoi N, Techasakul S. Cytotoxic and antimicrobial activities of aporphine alkaloids isolated from *Stephania venosa* (Blume) Spreng. *Planta Med.* 2011;77(13):1519-24.
58. Murphy PM. Chemokine receptors: cloning strategies. *Methods.* 1996;10(104-118).
59. Kim TK, Eberwine JH. Mammalian cell transfection: the present and the future. *Anal Bioanal Chem.* 2010;397(8):3173-8.
60. Sheikh S, Coutts AS, La Thangue NB. Transfection. *Basic science methods for clinical researchers.* London: Academic Press; 2017.
61. Hulme EC, Trevethick MA. Ligand binding assays at equilibrium: validation and interpretation. *Br J Pharmacol.* 2010;161(6):1219-37.
62. Schoofs G, Van Hout A, D'Huys T, Schols D, Van Loy T. A flow cytometry-based assay to identify compounds that disrupt binding of fluorescently-labeled CXC Chemokine Ligand 12 to CXC Chemokine Receptor 4. *J Vis Exp.* 2018(133).
63. Stoddart LA, White CW, Nguyen K, Hill SJ, Pflieger KD. Fluorescence- and bioluminescence-based approaches to study GPCR ligand binding. *Br J Pharmacol.* 2016;173(20):3028-37.
64. Zhu S, Meng Q, Schooley RT, An J, Xu Y, Huang Z. Structural and biological characterizations of novel high-affinity fluorescent probes with overlapped and distinctive binding regions on CXCR4. *Molecules.* 2019;24(16).
65. Nikfarjam L, Farzaneh P. Prevention and detection of mycoplasma contamination in cell culture. *Cell J.* 2012;13:203-12.

66. Duquenne C, Psomas C, Gimenez S, Guigues A, Carles MJ, Barbuat C, et al. The two human CXCR4 isoforms display different HIV receptor activities: consequences for the emergence of X4 strains. *J Immunol*. 2014;193(8):4188-94.
67. Gupta SK, Pillarisetti KJTJoI. Cutting edge: CXCR4-Lo: molecular cloning and functional expression of a novel human CXCR4 splice variant. *J Immunol*. 1999;163(5):2368-72.
68. Wu CH, Chang CP, Song JS, Jan JJ, Chou MC, Wu SH, et al. Discovery of novel stem cell mobilizers that target the CXCR4 receptor. *ChemMedChem*. 2012;7(2):209-12.
69. Fricker SP, Anastassov V, Cox J, Darkes MC, Grujic O, Idzan SR, et al. Characterization of the molecular pharmacology of AMD3100: a specific antagonist of the G-protein coupled chemokine receptor, CXCR4. *Biochem Pharmacol*. 2006;72(5):588-96.
70. Huang M, Giesler KE, Katzman BM, Prosser AR, Truax V, Liotta DC, et al. Small molecule CXCR4 antagonists block the HIV-1 Nef/CXCR4 axis and selectively initiate the apoptotic program in breast cancer cells. *Oncotarget*. 2018;9:16996-7013.
71. Harris DL, Mutz M. Debunking the myth: validation of fluorescein for testing the precision of nanoliter dispensing. *JALA*. 2016;11(4):233-9.

VITA

NAME	Thi Thai Ha Dinh
DATE OF BIRTH	24 Jan 1996
PLACE OF BIRTH	Viet Nam
INSTITUTIONS ATTENDED	Can Tho University
HOME ADDRESS	C151 Alley 15 Tran Van Hoai Street, Xuan Khanh Ward, Ninh Kieu District, Can Tho City, Viet Nam
AWARD RECEIVED	2020-2021 CU-ASEAN/NON-ASEAN Scholarship from Chulalongkorn University, Thailand



จุฬาลงกรณ์มหาวิทยาลัย
CHULALONGKORN UNIVERSITY